Summer 8-19-2022

Low Cost and Reliable Wireless Sensor Networks for Environmental Monitoring

Sonia Naderi
University of Maine, sonia.ndr.90@gmail.com

LOW COST AND RELIABLE WIRELESS SENSOR NETWORKS FOR ENVIRONMENTAL MONITORING

By

Sonia Naderi

MSc, Shahrood University of Technology, 2015

A DISSERTATION

Submitted in Partial Fulfillment of the

Requirements for the Degree of

Doctor of Philosophy

(in Electrical Engineering)

The Graduate School

The University of Maine

August 2022

Advisory Committee:

Dr. Ali Abedi, Professor of Electrical and Computer Engineering, Advisor

Dr. Walter Rawle, External Advisor

Dr. Rick Eason, Associate Professor of Electrical and Computer Engineering

Dr. Rosemary L. Smith, Professor of Electrical and Computer Engineering

Dr. Vincent Caccese, Professor of Mechanical Engineering

LOW COST AND RELIABLE WIRELESS SENSOR NETWORKS FOR ENVIRONMENTAL MONITORING

By Sonia Naderi

Dissertation Advisor: Dr. Ali Abedi

An Abstract of the Dissertation Presented
in Partial Fulfillment of the Requirements for the
Degree of Doctor of Philosophy
(in Electrical Engineering)
August 2022

This thesis utilizes wireless sensor network systems to learn of changes in wireless network performance and environment, establishing power efficient systems that are low cost and are able to perform large scale monitoring. The proposed system was built at the University of Maine's Wireless Sensor Networks (WiSe-Net) laboratory in collaboration with University of New Hampshire and University of Vermont researchers. The system was configured to perform soil moisture measurement with provision to include other sensor types at later stages in collaboration with Alabama A & M University.

In the research associated with this thesis, a general relay energy assisted scenario is considered, where a transmitter is powered by an energy source through both direct and relay links. An energy efficient scheduling method is proposed for the system model to determine whether to transmit data or stay silent based on the stored energy level and channel state. An analytical expression has been derived to approximate outage probability of the system in terms of energy and data thresholds.

In addition, we propose a model for evaluating the outage probability of a solar powered base station, equipped with a selected photo voltaic panel size and battery configuration. The energy harvesting environment location has been selected as the state of Maine, during a variety of weather conditions, considering base station loading during different days of the

week. Simulation results shows the required photo-voltaic panel size and number of batteries for specific tolerable outage probability of the system.

The fundamental contribution of this work is in development of hardware and software based on new methodologies to optimize network longevity using AI/ML. One of the most important metrics to define longevity and reliability is the outage probability of a network. We have derived equations for the outage probability, based upon power configuration panel size, battery capacity and the environmental factors, meteorological and diurnal. This will impact the observed cost function which is outage probability. The system models proposed in this thesis result in much more energy efficient systems with less outage probabilities compared to the current systems.

Keywords: Wireless Sensors Networks, Forest Models, Soil Moisture, Spectrum Sharing, Wireless Energy Transfer, Energy Harvesting, Relay-Assisted Communications, Harsh Environments, Green Communication, Cellular base station, Photo-Voltaic Panel, Battery, Markov Process, Outage Probability.

DEDICATION

I dedicate this dissertation to my lovely mother for her unconditional love and support.

You provided the best environment for me to grow and to be a better person.

I dedicate this dissertation to you.

ACKNOWLEDGEMENTS

I would like to express my greatest gratitude to my PhD advisor, Dr. Ali Abedi for all his advice and support during the last four years.

Also, I like to thank our sponsor, National Science Foundation (NSF) EPSCoR Track 2 program, our collaborators at the University of New Hampshire and University of Vermont, and University of Maine for sponsoring this research.

TABLE OF CONTENTS

LIST OF TABLES

LIST OF FIGURES

LIST OF ACRONYMS

Analog to Digital Converter (ADC)

Amplify-and-Forward (AF)

Additive White Gaussian Noise (AWGN)

Binary Phase-Shift Keying (BPSK)

Base Stations (BS)

Decode-and-Forward (DF)

Downlink (DL)

Energy harvesting (EH)

Integrated Circuitry (IC)

Line of Sight (LOS)

Least Significant Bit (LSB)

Long Term Evolution (LTE)

Micro Controller Unit (MCU)

Multiple Input Multiple Output (MIMO)

Probability Density Function (PDF)

Photo-Voltaic (PV)

Quality of Service (QOS)

Radio Frequency (RF)

Received Signal Strength Indicator (RSSI)

System Advisor Model (SAM)

Signal to Noise Ratio (SNR)

Uplink (UL)

Wireless Energy Transfer (WET)

Wireless Sensor Networks (WSN)

CHAPTER 1
INTRODUCTION

Measuring forest ecosystem properties and processes has become increasingly complex, involving a variety of data collection systems, software, and computing environments. Intelligent management of power and spectrum is the most important ingredient in wireless communications and in creating wireless sensor networks (WSN) [3, 4]. Sensor nodes, or small affordable devices with limited computational power and memory [5], may enable high-resolution forest ecosystem monitoring if they are integrated into a network that minimizes power consumption.

The problem of designing low cost wireless soil moisture sensor networks and sharing wireless spectrum in the forest ecosystem is considered in chapter 2. Chapter 3 is focused on relay-assisted wireless energy transfer scenarios for efficient spectrum sharing in harsh environments and forest areas. Then in chapter 4 of this thesis, we focus on outage probability optimization for solar powered cellular BSs, based on the number of batteries and PV panel size. Concluding remarks and future extensions of this work is provided in chapter 5.

A WSN to monitor soil moisture, which has been increasingly recognized as an important ecosystem property in forested and agricultural systems alike [6, 7, 8, 9, 10], inspiring the establishment of both soil moisture monitoring networks [11, 12, 13, 14] and large, freely available soil moisture databases [14] is very popular research topic [15, 16]. Despite the importance of measuring soil moisture and its distribution across the landscape [17], the cost of commercial soil moisture sensors remains prohibitive.

Wirelessly powered communication networks have been proposed as a new method which takes advantage of both information and energy carried by radio signals [18]. Wireless Energy Transfer (WET) for powering sensor nodes in the WSN, especially under extreme conditions, such as space applications and high temperature environments, has been attracting more and more interests recently from academics and industry [19, 20]. This involves the transmission

of electrical energy without wires using time-varying electric, magnetic, or electromagnetic fields and has been demonstrated as a viable option for various communication systems [21, 22].

5G is the fifth generation of cellular technology and everything is new in this technology such as new spectrum frequencies, new radio and new core network. 5G networks and their applications will be deployed in stages over the next several years to accommodate the increasing reliance on mobile and internet-enabled devices [23, 24, 25]. Simultaneous wireless information and power transfer have been introduced as a sustainable solution for 5G wireless communications [26, 27, 28].

Energy Harvesting (EH) has been recently developed as an efficient technique to minimize maintenance costs and extend lifetime of wireless networks. It can help to have more efficient wireless networks where network nodes periodically harvest energy from energy sources in their surrounding environment [29]. Recent advances in WET and its possibility of sharing energy leads to the concept of energy cooperation [30].

Relay-assisted communication techniques have drawn tremendous research interest in recent decades [31, 32, 33, 34]. This kind of communication is an efficient method for reliable data transmission, helps the severe propagation loss of wireless links and extends network coverage particularly in scenarios where source and destination are located far apart from one another. Their basic idea is allowing single-antenna devices to share their antennas and work collaboratively such that they construct a virtual Multiple Input Multiple Output (MIMO) system and create space diversity. As a result, the overall communication quality, including energy efficiency can be dramatically improved. The same concept applies to WET scenarios. The cooperation for energy transfer can be implemented to overcome the propagation attenuation caused by path-loss and channel fading. Energy-constrained relay node equipped with an energy harvesting device can harvest energy through the received Radio Frequency (RF) signal from the source.

The performance of cooperative networks aided by EH relay nodes in terms of outage behavior in slow fading scenario was investigated in [35]. The outage probability and the throughput of an Amplify-and-Forward (AF) relaying system using energy harvesting are analyzed in [36, 37]. Several power allocation strategies to optimize the outage probability in a Decode-and-Forward (DF) cooperative network where multiple source-destination pairs communicate via a shared energy harvesting relay is proposed in [38]. In [39], a harvest then cooperate protocol was proposed in a cooperative network where a source and AF based relay harvest energy from a hybrid access point in the Downlink (DL) and cooperate in the Uplink (UL) for the source information transmission. The approximate expression of the average throughput was derived for Rayleigh fading channels.

Currently available off the shelf equipment provide continuous or periodic pulsed energy and data transmission which is not an ideal scheme due to the stochastic nature of wireless channels. Recently, a novel stochastic model for two separate data and energy channels and a new transmission scheduling were proposed in [40]. However, there is no work which studies outage probability performance of relay-assisted energy transmission scenario which in addition to direct link, EH relay helps energy source to power a transmitter which is attempting to send data to a destination based on energy efficient transmission scheduling.

In this thesis, we model fading wireless channels for power and data separately and transmit energy and data randomly based on two separate stochastic models for data and energy channels [41]. We investigate the effects of energy efficient scheduling methods on wireless sensor outage. This method can determine when to transmit data based on the stored energy level in the sensor and the noise levels on the data channel. If the sensor has a low level of energy and the data channel has a high level of noise it would be best to wait until either the sensor has more energy or the channel has less noise in order to avoid wasting energy and losing data. We consider Additive White Gaussian Noise (AWGN), Rayleigh and Rician channel models for static or mobile system nodes. We will set a threshold on required transmission energy and channel quality to decide whether the transmission is beneficial or

risky and calculate the outage probability of the system. Outage probability of a system including sensor energy and data outage and its relationship with energy and data threshold will be derived analytically and verified by simulations.

Developing countries currently contribute to the bulk of the worldwide growth in cellular networks [42]. In many such countries, reliable grid power is not available and many of the cellular Base Stations (BS) are operated by on-site fossil fuel (e.g. diesel) based generators [43]. In addition to increasing the pollution levels, they are also susceptible to variations in energy costs. In such scenarios, solar powered cellular BSs are a viable and attractive alternative. In addition, solar powered BSs may also be used in places where reliable grid power is available in order to reduce the energy costs and the carbon footprint of cellular networks.

Cellular BSs are important parts of WSN that need to be considered in our work. The number of cellular BSs and cellular subscribers has been increasing rapidly which results in high amount of energy consumption and carbon footprint cased by such a systems [44]. There are 43000 solar powered BSs around the globe based on a report in 2014 consuming great amount of energy in cellular networks [45, 46]. Solar powered BSs are very popular since they extend the cellular coverage and decrease the Carbon footprint by using renewable energy [47]. These kind of BSs harvest solar energy during the day by using Photo-Voltaic (PV) panels for their operations. The excess power will be stored in their batteries for their night time operations and bad weather days.

In this thesis, we address the problem of designing and provisioning solar powered cellular nodes in terms of the required battery capacity and PV panel size, with the objective of decreasing the power outage probability and minimizing the system cost by considering the tolerable outage probability of the system. Solar powered BSs are currently under development and deployment by a number of operators. For example, Orange has multiple deployments in the Middle East and Africa, while NTT DOCOMO in Japan and Grameenphone in Bangladesh are in various stages of deployment [48, 49]. While the initial experimental

deployments serve as a proof of concept, a number of open problems still remain before "zero energy networks" become a reality [48]. The most fundamental of these problems include the dimensioning of solar powered BSs in terms of their EH and storage, design of routing and data transmission strategies, and strategies to guarantee uninterrupted service while minimizing energy consumption. While existing literature has investigated some aspects of this problem, the problem of resource dimensioning remains open. In [48] the authors obtain the minimum required PV wattage and battery sizes for solar powered BSs by using the historical data of solar radiation in the Typical Meteorological Year (TMY) for a given location. In particular, the TMY data for the worst month is chosen to determine the PV wattage and number of batteries. Such an approach is not necessarily cost optimal. Also, due to seasonal variations over the years, TMY data is not very reliable when it comes to dimensioning a PV system. In other works [50], the authors model solar powered BSs, but do not use the long term weather data. Furthermore, the model presented only provides an estimate of the PV panel and battery dimension, and does not provide the cost optimal solution for a given outage probability.

The PV panel size and number of batteries are always the challenging part of designing these BSs since appropriate design results in significantly decreasing the cost of the system. Using large panel size and more batteries makes the system of course more reliable but on the other side much more expensive. The small panel size and fewer batteries results in more system outage and less system reliability as well. System outage occurs when BS does not have enough energy for its operation. Frequent system outage causes bad Quality of Service (QOS) for customers and results in wasting of resources.

Finding the optimal PV panel size and number of batteries to keep the system outage more than a specific tolerable threshold is a challenging part of designing such cellular systems. The optimal configuration is a configuration with the least cost that satisfies operator power outage considerations of the system [47]. In order to solve this problem,

outage of the system should be calculated in terms of the PV panel size and number of batteries.

In recent literature, the problem of power outage probability in terms of different system parameters such as BS battery level is considered. Battery level at the BS is modeled by a discrete time Markov chain. A closed term expression for outage probability is derived for different states in the considered model. Dimensioning guidelines are important aspects of such a systems and are considered in [51, 52, 53, 54, 55, 56, 57, 58]. Authors in [59, 60] used long term solar irradiation data for resource cost optimal dimensioning in cellular BSs. Some literature considered simulation based approaches using commercial software but these methods are very time consuming from computation aspects and do not provide the performance of the system for design purposes [61].

Authors in [62] modeled energy storage in BS with Markov chain and solar irradiation exhibiting exponential distribution. Modeling the solar energy in solar powered BSs as a Markov process has been used to great extent in the recent literature [63, 64]. Markov models are used in [65] for modeling solar energy collection PV panel size and number of batteries required are determined in a cost optimal way.

To the best of our knowledge, there is no work that considers the problem of outage probability calculations of solar powered BS in terms of BS load, battery level and harvested solar energy in the U.S. state of Maine. In the last chapter of this thesis, we propose a model for evaluating the outage probability of solar powered BS based on the PV panel size and number of batteries for harvested solar energy by BS in the U.S. state of Maine during different weather conditions and BS load during different days of the week. We evaluate the performance and accuracy of the proposed system in different conditions by simulation and find the required PV panel size and number of batteries for specific tolerable outage probability of the system.

CHAPTER 2

SHARING WIRELESS SPECTRUM IN THE FOREST ECOSYSTEM

2.1 Background

Measuring forest ecosystem properties and processes has become increasingly complex, involving a variety of data collection systems, software, and computing environments. Intelligent management of power and spectrum is the most important ingredient in wireless communications and in creating WSNs with high reliability and longevity. The main application under study in this chapter is accurate monitoring of forest ecosystems using high spatio-temporal resolution. The high cost of current systems and their power consumption limits wide spread use of these systems limiting the accuracy of current models.

A sensor network is a group of sensors where each sensor monitors data in a different location and sends that data to a central location for storage, viewing, and analysis. Sensors do communicate with each other using network level protocols to avoid interference and unnecessary spectrum pollution, and to adjust their power level. They also act as relays for sensors not reachable by the BS. That is why we call them networks. We have deployed a wireless sensor network to monitor physical or environmental conditions such as soil moisture at this phase and air temperature, relative humidity and soil temperature in the future phases. These sensors will cooperatively pass data through the network to a centralized processing location or act on the information in a distributed manner. A wireless soil moisture sensor network refers to a WSN that is comprised of a network of soil moisture sensors. These networks are bidirectional and also allow control of sensor sampling rate and transmit/sleep state.

We focus on producing power efficient systems that are low cost to enable large scale soil moisture monitoring. The proposed system was built at the University of Maine's Wireless Sensor Networks (WiSe-Net) laboratory in collaboration with University of New Hampshire

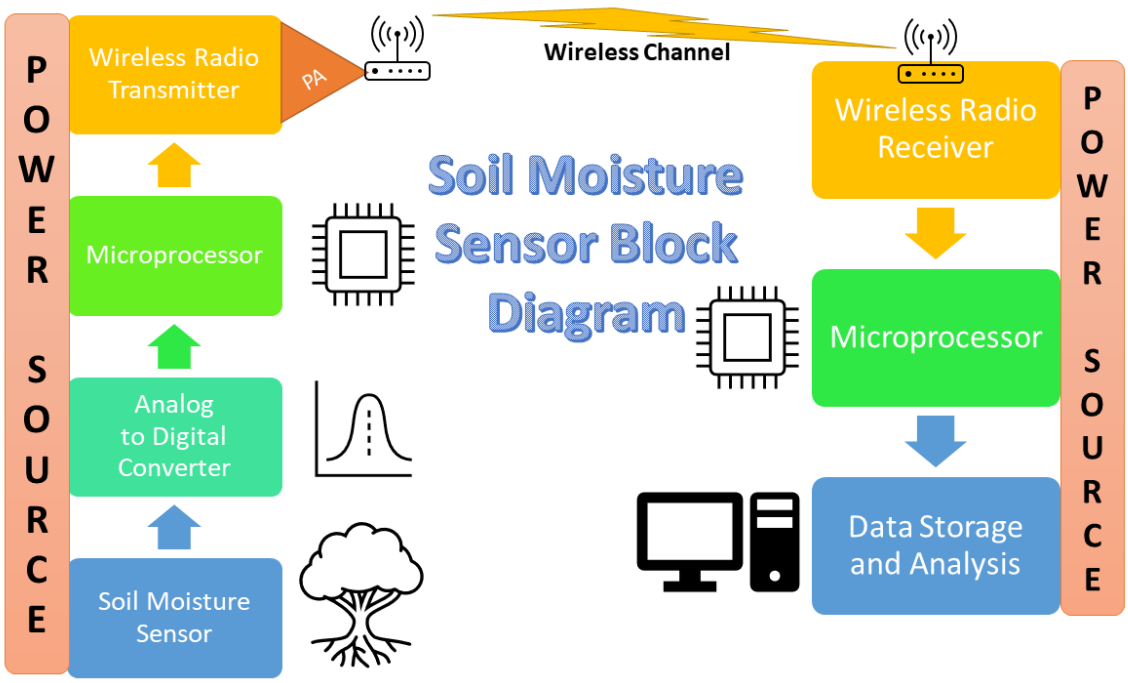

Figure 2.1. System Block Diagram

and University of Vermont researchers to perform soil moisture measurement with provision to include other sensor types at later stages.

2.2 System Model

Figure 2.1 shows the system block diagram of the proposed soil moisture sensing system. Each block is explained in the following subsections.

A. Soil Moisture Sensor

One important factor affecting the growth rate of forests is the available moisture in the soil [9]. In addition to the availability of water for the plants themselves, the level water in the soil affects the usage of nitrogen uptake by the roots and the oxygen level at the roots [66].

The standard way to determine soil moisture is the thermogravimetric method which is introduced in [67]. In this method, the weight loss of soil is measured after oven drying of

soil with known mass at 105° C. The main issues with this method are that they are very time consuming and they can not be repeated because they are destructive measurements.

Over the past several decades, these destructive methods have been replaced by electronic devices such as capacitance, impedance, dielectric and time domain reflectrometry sensors [68]. Different soil moisture measurement techniques have been proposed in the literature [69, 70, 71]. For instance in [71], the authors proposed a way for measuring soil moisture content by monitoring electromagnetic radiation of soil, which depends on sensitivity of microwaves to soil moisture. Impedance soil moisture sensing technology involves inserting separate rods into the soil and changing conductivity by altering water content [72]. This method is based on changing the soil conductivity by changing the water content of the soil. Frequency domain sensors has been proposed in [73]. These kinds of soil moisture sensors measure soil impedance changes because of the water content variations. These sensors are available as single and multi sensor probes which offer different measuring techniques [74, 75]. Other methods include fiber optic sensors [76, 77], dye doped plastic fibers [78], ceramic sensors [79], and neutron scattering method [80].

There are two types of soil moisture sensors, contact-based and contact-free. In the contact-based method, the detection area of the sensor needs to be touched directly with the detection media, i.e., the soil. Contact-based soil moisture sensors have various methods based on detection parameters such as capacitive soil moisture sensors [81], heat pulse sensors, and fiber optic sensors [82]. With contact-free soil moisture sensors, there is no need to contact the detection media that is being detected. Contact-free soil moisture sensors include passive microwave radiometers, synthetic aperture radars, and thermal methods [83, 84]. Contact-free soil moisture sensors are more expensive and more complicated compared to contact-based soil moisture sensors.

In this thesis, we are using the DFRobot SKU:SEN0193 which measures soil moisture levels by capacitive sensing rather than resistive sensing, which is more durable, stable, and most importantly employs low power. It is made of corrosion resistant material and includes

an on-board voltage regulator with an operating voltage range of 3.3–5.5 V enabling easy connection to a low voltage microprocessor with support for both 3.3 V and 5 V. This was selected over the Adafruit STEMMA I2C Capacitive Moisture Sensor capacitive soil moisture sensor and the Grove Capacitive Soil Moisture Sensor based on the criteria outlined above.

B. Analog to Digital Converter (ADC)

Since the selected sensors are analog devices, it is necessary to convert the sensor output to digital format, readable by the microprocessor that can only accept digital inputs.

We need to make judicious decisions in measurement scheduling, i.e., when is the best time to take a measurement, so as to minimize the total amount of time the node needs to be active in actuating the moisture probes and in data transmission, while still satisfying the monitoring objective, i.e., achieving a desired level of accuracy (as determined by the ecological models) in the estimated soil moisture evolution using the measurement data collected.

The output values of soil moisture sensor varies from 0 to 100 representing the lowest and highest soil moisture, respectively. The Texas Instruments Launchpads has 12-bit ADC and its sampling rate is 200 ksamples/s. It means the resolution or the number of intervals of this ADC is equal to 4096 and the dynamic range is 72dB. The least significant bit (LSB) can be calculated as full scale range of the sensor output voltage divided by number of intervals which is 4096. Since the sensor output values vary between 0 and 100, the LSB is equal to 0.024 and the quantization error in our ADC is around 0.012. In general we expect the power consumption of the ADC to increase as the accuracy of the ADC is increased, since the sampling rate is increasing.

C. Microprocessor

The computational logic is responsible for handling the on-board data processing and manipulation, temporary storage and data encryption. The faster and more powerful processors usually have a higher energy consumption and cost. Processors with high code density and

different operational modes like active, idle, nap and sleep modes to preserve energy are required.

There are different microprocessor options such as Intel 8051, Microchip PIC, Atmel AVR and TI ARM. Among these microprocessor options, ARM processors are widely used in consumer electronic devices. Because of their reduced instruction set, they need fewer transistors, which enable a smaller die size of the integrated circuitry (IC). The ARM processors' smaller size and lower power requirements makes them suitable for increasingly miniaturized devices.

In this research, we are using Texas Instruments CC1310 device which is a wireless microcontroller unit (MCU) with an ARM Cortex-M3 microprocessor. The ARM Cortex-M3 processor is a 32-bit processor for low-cost high performance applications. The ARM Cortex-M3 processor family was selected because they are optimized for cost and are energy-efficient. These processors have been used in a variety of applications, including a variety of edge devices, industrial control, and everyday consumer devices. The processor family is based on the M-Profile Architecture that provides low-latency and high reliability in embedded systems. The Cortex-M3 processor provides a high-performance, low-cost platform that meets the system requirements for low-power consumption and high reliability.

D. Radio Module

Radio modules are required to enable sensor nodes to communicate with each other and to the base station. We are using a Sub 1 GHz radio module which provides a reliable transceiver with one built-in antenna at a reasonable cost. Sub 1 GHz RF operates in the ISM spectrum bands below 1 GHz – typically in the 769 – 935 MHz , 315 MHz and the 468 MHz frequency range. They offer more range than the 2.4 GHz. Sub 1 GHz wireless transmission offers 1.5-2 times more distance coverage than the 2.4 GHz spectrum. Also, the Sub 1 GHz wireless spectrum has a long range mode that is well suited to this application. Wireless Sub 1 GHz RF needs a lower power signal from the transceiver compared to the 2.4 GHz spectrum to get the same output power signal at the receiver.

Antenna Option	Directivity	Effective Radiated Power
2	3.92dBi	46.61%
3	4.13dBi	63.05%
4	4.39dBi	31.33%
5	4.16dBi	46.83%
On-board Antenna	4.47dBi	80.38%

Table 2.1. Antenna Metrics [1]

2.3 Simulation Results

In this section experiment design and obtained results are presented. Antenna test results are presented first, followed by overall system verification results.

A. Antenna Test Results

Five antenna types were considered. Each antenna was subjected to the same range testing. However Antenna 1, a CR2032 PCB Antenna, had such a poor overall performance, such that it was irrelevant to include in this research (Table 2.1).

Especially in regards to power efficiency, this provides close, but not exact expectations of the system. Antenna 3, a compact PCB helical antenna, and antenna 4, an orthogonal arrays of two helical antennas, performed similarly in range testing. Antenna 5 was the worst performing, with a range of under 100 feet before falling below a level that was unreadable. Using a Received Signal Strength Indicator (RSSI) cut of value of 75 dBm, the board antenna achieved a working distance of 250 ft, and for now, we will use the 250 ft. result to design our network grid.

Figure 2.2 shows RSSI of each antenna at each distance measured. A few data points are higher than there previous ones in the figure and there are a few things that could be causing it to happen. It could be a stronger signal, but that is wrapped up in antenna radiation patterns, multipathing, etc. Also, this happens because of the scattering effects in the forest.

Future designs will implement a compact PCB helical antenna, demonstrated with antenna 3, as it allows for the possibility of increasing the current 250 ft. range and reducing the overall size of the device.

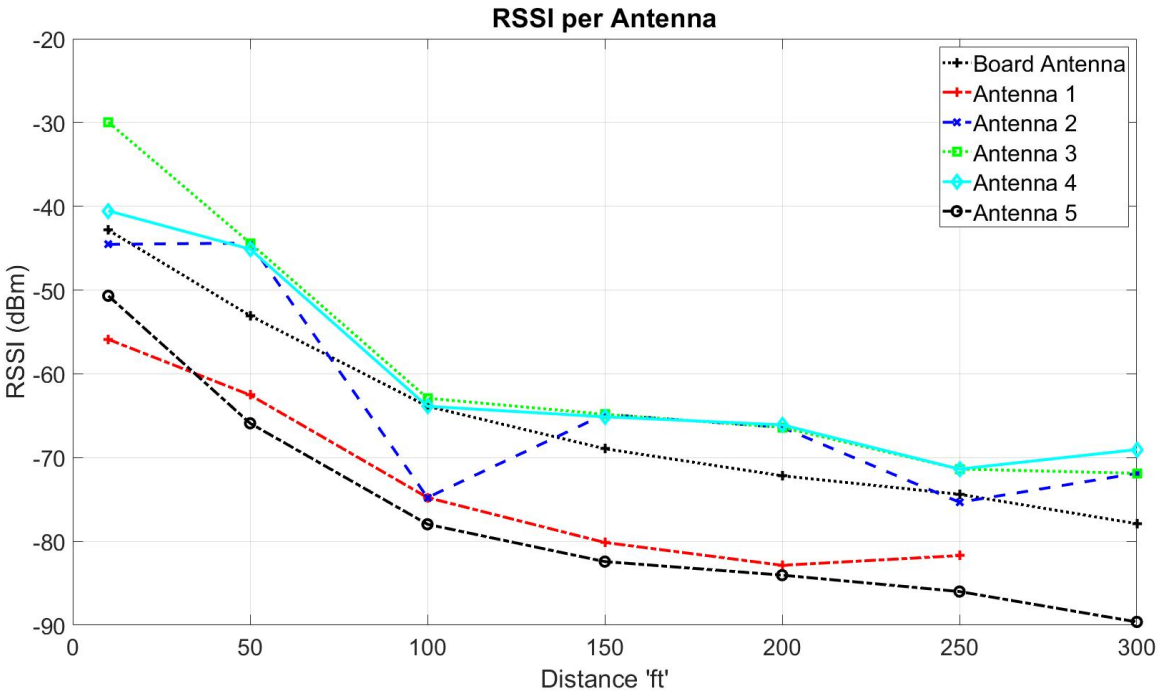

Figure 2.2. RSSI of each antenna at each distance measured

Each antenna was tested using the same methodology. Matching antennas were attached to the base station, and a separate TI launchpad. This launch pad was programmed to transmit one hundred packets of random characters at multiples of fifty feet distances to a final three hundred foot range. The base station, consisting of another TI launchpad and a laptop computer, recorded each incoming packet's RSSI at each distance. Antenna 3, the compact helical antenna will be the antenna used in future designs. It outperformed the current built-in antenna, and while it was slightly under performing as compared to the orthogonal compact PCB antennas, the slight increase in performance did not warrant the dramatic increase in antenna size. More antenna tests are in Appendix A.

B. Sensor Calibration

The deployed system is shown in figure 2.3. The system's sensors were calibrated to correct the hysteresis in the sensor response. To do this, data was collected using a Campbell Scientific data logger with a CS650 Campbell Scientific soil moisture sensor deployed as

Figure 2.3. Proposed low cost sensor deployment

Figure 2.4. Calibration was done following [85, 86] using Gaussian Process Regression. A Gaussian process is a non-parametric tool for learning scalar regression functions from sample data. A Gaussian process describes a stochastic process in which the random variables, in this case the outputs of the modeled function, are jointly Gaussian distributed [85].

The soil for the experiment was dried in an oven at 225°F (107°C) for one hour. The data was collected by placing the two sensors in the same soil approximately 2 cm apart. Water was then added to the soil in increments of 15 ml every five minutes until 300ml was added. Both sensors were sampled once per second. The collected data was then divided into training (90%) and test data (10%).

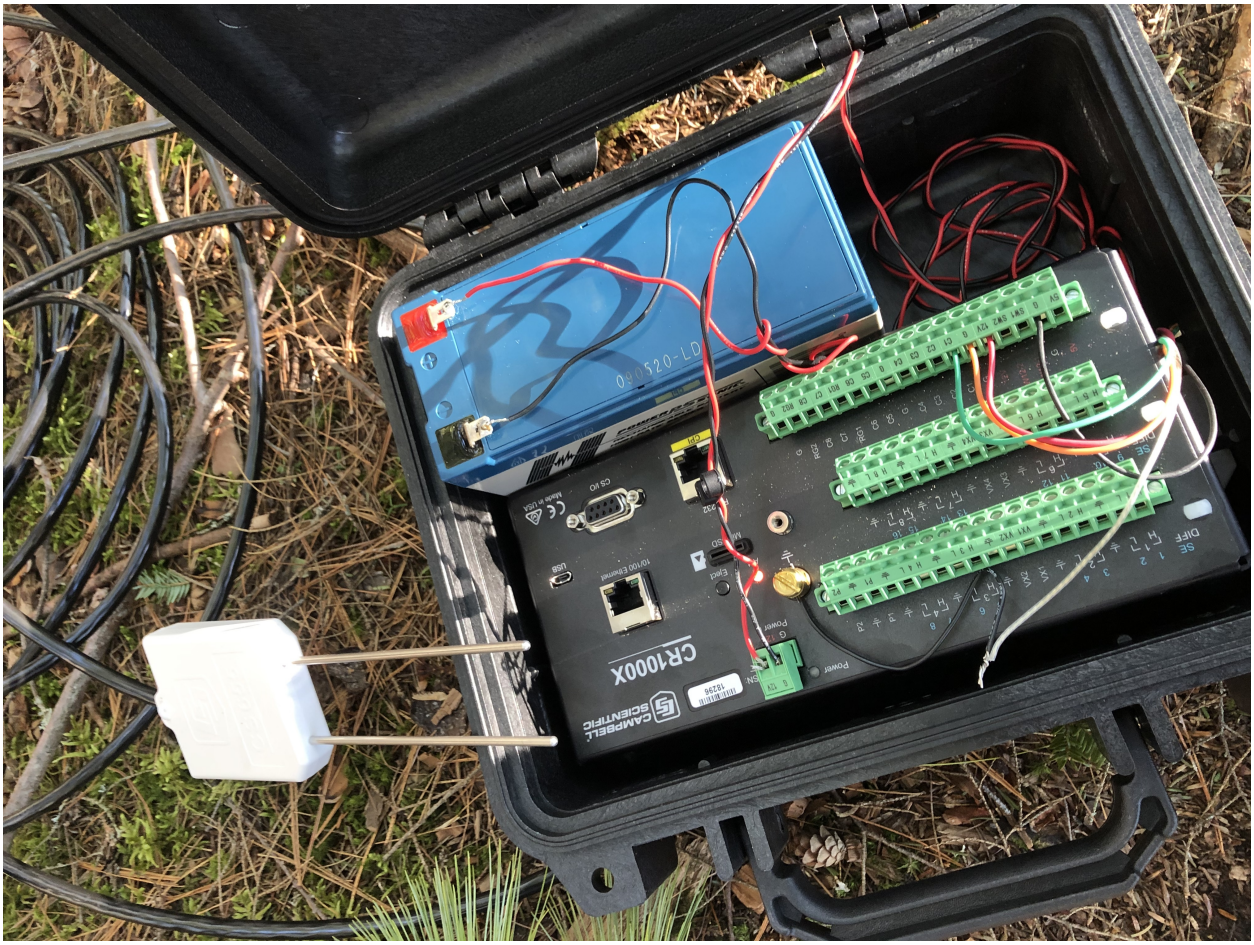

Figure 2.4. Campbell Scientific sensor deployment

A comparison of the base sensor data and the true values can be seen in figure 2.5. After calibration, the sensor values closely tracked the true values, as shown in figure 2.6. All values assume the Campbell Scientific data logger values as the ground truth values. Computations were completed using methods described in [87, 88, 89]. Each experiment included multiple points in the lab environment with no environmental control such as fixed temperature or humidity, that results in a spear of points. We also mapped the points to the similar scale as the calibrated sensor which also resulted in more non-linearity.

Basically the spread of values is large because of measurement noise (the sensors are low quality), the time-alignment of the two time series is not perfect leading to variance in the figures. The area around 600 in figure 2.5 could be samples that are due to the temporal

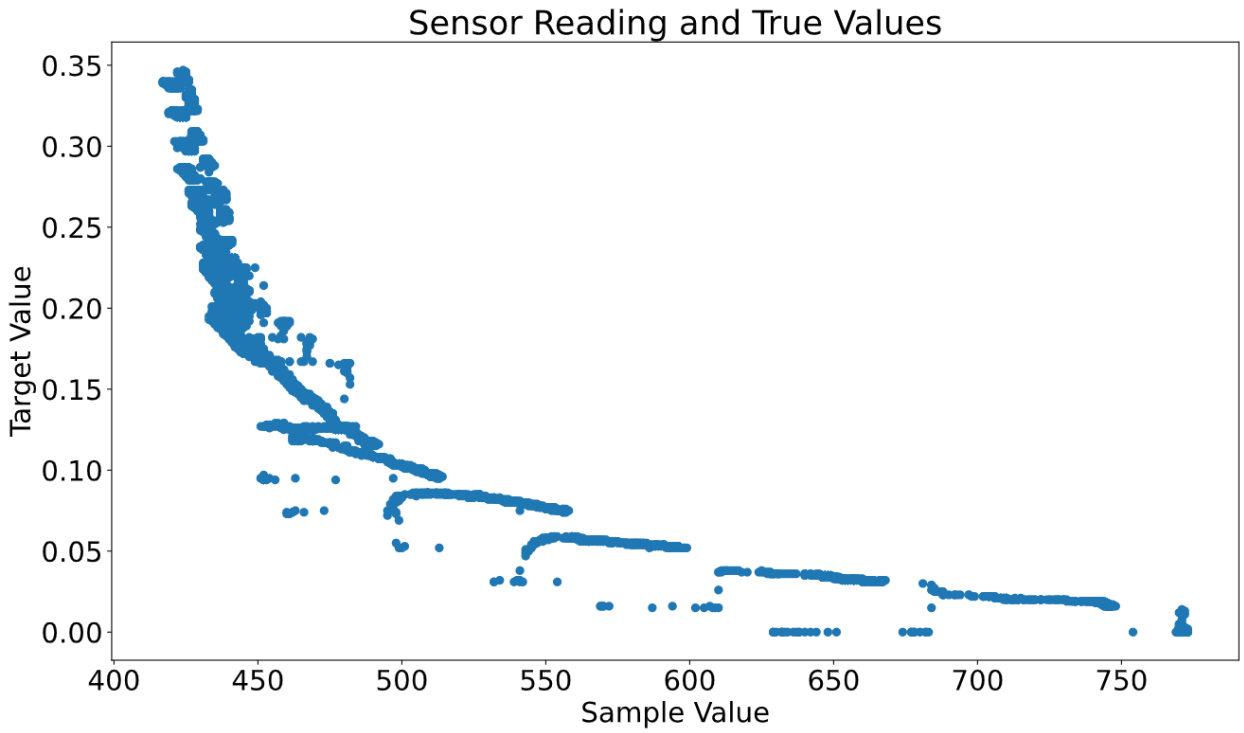

Figure 2.5. Target value versus sample value

misalignment, but more likely it's because there is a spike in the sensor reading when the water is added, then it's absorbed into the soil and the reading falls. It could be that the lower values are from different readings (when the values were actually higher). All of these error sources carry over to the model. Since there is a lot of variance, there is not way it is all explained by the Gaussian Process. In fact, the model is pretty significantly over fit, which is artificially reducing the variance.

2.4 Concluding Remarks

In this chapter, a low cost and reliable wireless soil moisture sensing system is proposed to enable high spatio temporal data collection for improving our understanding of forest ecosystems. The developed methods allow for implementation of low-power sensor networks with optimized control. We compared the proposed system with industry standard wired systems in a field experiment. The results show reasonably similar data at much lower

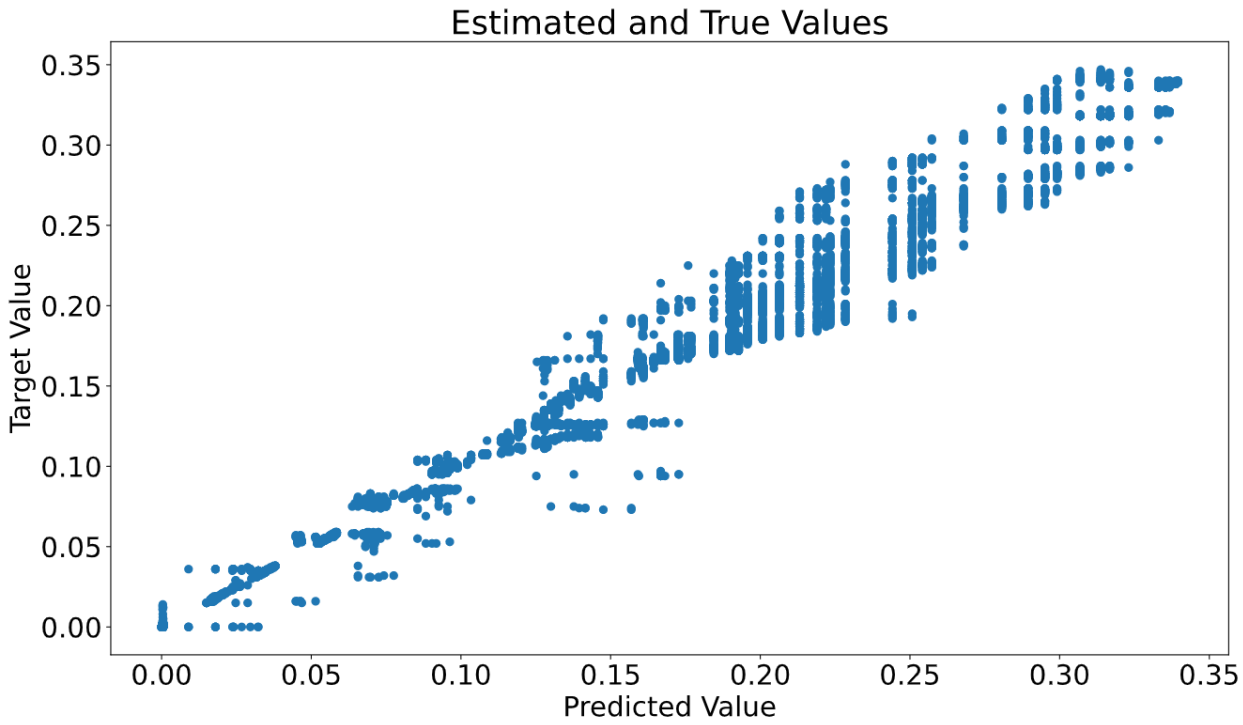

Figure 2.6. Target value versus predicted value

cost. Future work includes enhancing the sensor node with additional sensor types (soil and ambient temperature, snow depth, and more) and scaling up the network with more sensor nodes [90, 66].

The result of this chapter has been published in the following journal and conference:

- S. Naderi, K. Bundy, T. Whitney, A. Abedi, A. Weiskittel, and A. Contosta, "Sharing Wireless Spectrum in the Forest Ecosystems Using Artificial Intelligence and Machine Learning," International Journal of Wireless Information Networks (IJWIN), Aug 2022, pp. 1-12.

- T. Whitney, T. Nicholas, S. Naderi and A. Abedi, "A Low Cost Power Efficient Wireless Soil Moisture Sensor Network for Forest Ecosystem Monitoring," 2020 IEEE MIT Undergraduate Research Technology Conference (URTC), Oct 2020, pp. 1-4.

CHAPTER 3

RELAY-ASSISTED WIRELESS ENERGY TRANSFER FOR EFFICIENT SPECTRUM SHARING IN HARSH AND FORESTRY ENVIRONMENTS

3.1 Background

With the exponential growth in the number of wireless devices and limited available spectrum, the problem of spectrum sharing remains in the forefront of the research community. Due to the large number of wireless sensing devices, even a small percentage of savings can translate into significant spectrum efficiencies. One of the main hurdles in efficient spectrum sharing in WSN is the problem of power management at the node level to promote longevity without polluting the spectrum, while promoting collaboration. This problem is even more challenging in extreme (harsh) environments where access to power and battery replacement and charging is limited, if not impossible. Passive sensor technology can be used to eliminate the need for batteries, but it suffers from short communication range.

Recently, WET for powering remote sensor nodes in a WSN has drawn considerable research attention, since it can charge sensing circuits remotely and relieve the need for battery replacement. Modeling the charging and power utilization processes can help with smart transmission decisions, which can eliminate unnecessary transmissions and not only save limited battery power at the node level, but also efficiently utilize the shared spectrum.

Relay-assisted communication techniques have drawn tremendous research interest in recent decades [31, 32, 33]. This kind of communication is an efficient method for reliable data transmission, helps the severe propagation loss of wireless links and extends network coverage particularly in scenarios where source and destination are located far apart from one another. Their basic idea is allowing single-antenna devices to share their antennas and work collaboratively such that they construct a virtual MIMO system and create space diversity. As a result, the overall communication quality, including energy efficiency can be dramatically improved. The same concept applies to WET scenarios. The cooperation

for energy transfer can be implemented to overcome the propagation attenuation caused by path-loss and channel fading. Energy-constrained relay nodes equipped with an energy harvesting device can harvest energy through the received RF signal from the source.

The performance of cooperative networks aided by EH relay nodes in terms of outage behavior in slow fading scenarios was investigated in [35]. The outage probability and the throughput of an AF relaying system using energy harvesting are analyzed in [36, 37]. Several power allocation strategies to optimize the outage probability in a DF cooperative network where multiple source-destination pairs communicate via a shared energy harvesting relay is proposed in [38]. In [39], a harvest then cooperate protocol was proposed in a cooperative network where a source and AF based relay harvest energy from a hybrid access point in the DL (link from the base station to the user) and cooperate in the UL (link from the user to the base station) for the source information transmission. The approximate expression of the average throughput was derived for Rayleigh fading channels.

Currently available off the shelf equipment provide continuous or periodic pulsed energy and data transmission which is not an ideal scheme due to the stochastic nature of wireless channels. Recently, a novel stochastic model for two separate data and energy channels and a new transmission scheduling protocol were proposed in [40]. However, there is no work which studies outage probability performance of relay-assisted energy transmission scenario which in addition to direct link, EH relay helps energy sources to power a transmitter which is attempting to send data to a destination based on energy efficient transmission scheduling.

In this chapter of the thesis, we consider a general relay energy assisted scenario, where a transmitter is powered by an energy source through both direct and relay links. We model data and energy channels separately, transmit energy to power the transmitter battery and schedule data transmission based on stochastic models for data. We also consider various static, mobile and highly scattered channel models. We will set a threshold on required transmission energy and channel quality to decide whether the transmission can be successful (efficient use of spectrum) or the packet may not reach the destination (polluting

the spectrum unnecessarily). An energy efficient scheduling method is proposed for the system model to determine whether to transmit data or stay silent based on the stored energy level and channel state. An analytical expression has been derived to approximate outage probability of the system in terms of energy and data thresholds. All theoretical results are simulated which verify the effectiveness of energy relaying and the proposed energy efficient scheduling method in reducing the outage probability of the system.

3.2 System Model

Throughout this thesis, we use subscript-S for source, subscript-T for transmitter, subscript-R for relay and subscript-D for destination. As shown in figure 3.1, this work considers a WSN scenario that consists of four point to point channels including S-T, S-R, R-T and T-D pairs. The considered model transfers information from a transmitter terminal, T, to a destination terminal, D. We assume that the transmitter T is powered by an external energy source, S via direct link. Direct link refers to point-to-point transmission in which there is only one channel without any relay between transmitter and receiver. Energy transfer from the source S to the transmitter T is also assisted by a relay denoted by R. As a result, the transmitter T receives energy from two separate direct and relay links. All these devices are assumed to have only a single antenna in this work. Let $\widetilde{h}_{XY}$ denote the channel coefficient from X to Y with $X, Y \in \{\mathrm{S}, \mathrm{T}, \mathrm{R}, \mathrm{D}\}$. Thus, the channel power gain from X to Y can be defined as $h_{XY} = |\ \widetilde{h}_{XY}\ |^2$ which $|.|$ denotes the absolute value operation [91]. We assume channel gains remain constant during each transmission block (denoted by T) but change independently from one block to another. Also, each transmission block is further divided into a number of time slots.

In this thesis, we use the idea of modeling data and energy channels separately proposed in [40] and analyze adding a relay-assisted energy transmission scenario. Depending on the existence of static or mobile nodes, we consider three different channel models. For static channels where both nodes associated with one link are fixed, we consider an AWGN channel

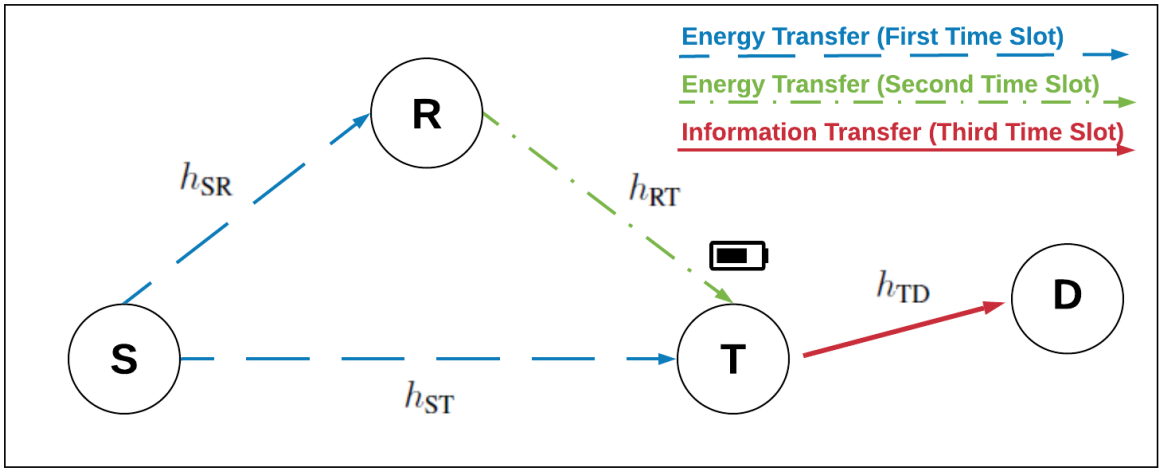

Figure 3.1. Relay-assisted energy charging model.

model with a Probability Density Function (PDF) of a normal distribution $f(x)$ as follows [92]

$$f(x) = N(\mu, \sigma^2) = \frac{1}{\sqrt{2\pi\sigma^2}} e^{-(x-\mu)^2/2\sigma^2} \tag{3.1}$$

$$\sigma = \sqrt{10^{-\frac{SNR}{10}}} \tag{3.2}$$

where μ and σ are the mean and variance of an AWGN channel respectively and SNR denotes signal to noise ratio. In cases that we have relatively mobile nodes, we use Rayleigh and Rician channel models in highly scattered environments without and with Line Of Sight (LOS) with their PDFs as follows [92]

$$g(y, \sigma^2) = \frac{y}{\sigma^2} e^{-\frac{y}{2\sigma^2}} \tag{3.3}$$

$$h(z, \sigma^2) = \frac{z}{\sigma^2} e^{-(z^2+v^2)/2\sigma^2} I_0(\frac{zv}{\sigma^2}) \tag{3.4}$$

where v is Rician channel parameter and $I_0(.)$ is the modified Bessel function with zeroth order. For simplicity in two cascaded channels calculations, we model S $\rightarrow$ R and R $\rightarrow$ T channels with AWGN channel model and study 9 different scenarios considering that S $\rightarrow$ T and T $\rightarrow$ D channels may fall under one of these three channel models.

3.3 Proposed Energy Efficient Transmission Scheduling

As demonstrated in the system model section, our model consists of two transmission phases. In the first phase, which is providing energy for the transmitter T, the source S sends energy to the transmitter T over direct link. This can also be overheard by relay R due to the broadcasting nature of wireless communication. In addition, the relay is assumed to have no other embedded energy supply or is not willing to use its own energy for this communication. Thus, it needs to first harvest broadcasted energy by the source S, use a portion of this energy for its own operation, and then redirect the remaining harvested energy toward the transmitter T. In the second phase, the powered transmitter T tries to send data to the destination D. The proposed relay-assisted transmission block in this work is shown in Figure 3.2. In each transmission block of time duration T, the first τT amount of time with $0 < \tau < 1$ is assigned to the energy transfer phase from the source S to the transmitter T and relay R. For simplicity of formulation, we follow a similar approach as [39] by selecting equal time slots for sending energy from the source S to the transmitter T and relay in the first time slot and from relay node to the transmitter T in the second time slot.

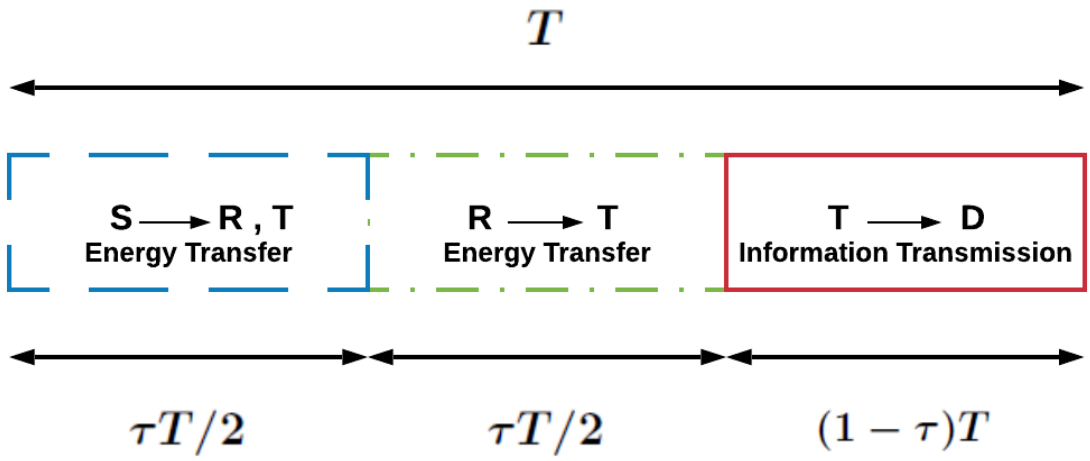

Figure 3.2. Three time slot energy transfer and data communication.

Thus, this fraction of the block is further divided into two time slots with an equal length of $\tau T/2$ as shown in Figure 3.2. The remaining fraction $(1-\tau)T$ of the block is for the second phase which is data transmission from the transmitter T to the destination D over the third time slot. We also assume that the channel state does not change significantly from one time slot to the next and estimate the wireless channel status in each time slot and using that estimate for the next time slot.

In this thesis, we use a decision algorithm to avoid transmission of data when the channel is in low SNR or deep fading and battery energy is less than the minimum required energy for transmission. We set a threshold on energy and channel quality in the data transmission phase to decide whether the transmission in this time slot is beneficial or risky. This threshold is determined offline based on the channel model. It is obvious that outage can be significantly increased if the transmission is carried out over the channel with SNR below the defined threshold. In the case that the transmitter T attempts to transmit data when data channel state is in poor quality state and battery level is very low, there is a very low chance that the destination receives transmitted data error free. As a result, by this approach and avoiding risky transmission of data, we can decrease the outage probability of the system and prevent wasting battery energy.

In the next sections, we will analyze outage probability expressions in the proposed system. We show that using the proposed relay-assisted energy transmission scheme for WET will decrease the outage probability of the system.

3.4 Analytical Outage Probability

Since the power and data channels are independent, the probability of an outage occurring in the proposed relay-assisted scenario is as follows [41]

$$\text{Prob(system outage)} = (\mathrm{P}_{\mathrm{R}}^{\mathrm{E}}) \times \left[\bar{\mathrm{P}}_{\mathrm{T}}^{\mathrm{E}} + (1 - \bar{\mathrm{P}}_{\mathrm{T}}^{\mathrm{E}}) \times (\bar{\mathrm{P}}_{\mathrm{T}}^{\mathrm{D}}) \right] + (1 - \mathrm{P}_{\mathrm{R}}^{\mathrm{E}}) \times \left[\overset{\triangle}{\mathrm{P}}_{\mathrm{T}}^{\mathrm{E}} + (1 - \overset{\triangle}{\mathrm{P}}_{\mathrm{T}}^{\mathrm{E}}) \times (\overset{\triangle}{\mathrm{P}}_{\mathrm{T}}^{\mathrm{D}}) \right] \tag{3.5}$$

where $\mathrm{P_R^E}$ is energy outage probability at the relay node, $\bar{\mathrm{P}}_{\mathrm{T}}^{\mathrm{E}}$ is energy outage probability at the transmitter node when there is outage at the relay node, $\bar{\mathrm{P}}_{\mathrm{T}}^{\mathrm{D}}$ is data outage probability at the transmitter node when there is outage at the relay node, $\overset{\triangle}{\mathrm{P}}_{\mathrm{T}}^{\mathrm{E}}$ is energy outage probability at the transmitter node when there is no outage at the relay node and $\overset{\triangle}{\mathrm{P}}_{\mathrm{T}}^{\mathrm{D}}$ is data outage probability at the transmitter node when there is no outage at the relay node. This equation can be calculated using relevant equations in this chapter.

In this work, we assumed that S $\rightarrow$ R and R $\rightarrow$ T channels are modeled using AWGN channel model and S $\rightarrow$ T and T $\rightarrow$ D channels may fall under one of three channel models. Based on that, we will have 9 different channel model combinations. We derived outage probability for the case that we have AWGN-AWGN-Rician-Rayleigh channels for S $\rightarrow$ R, R $\rightarrow$ T, S $\rightarrow$ T and T $\rightarrow$ D links respectively and will consider other possible scenarios in simulation part. The existing integrals in equations can be evaluated numerically to provide the outage probability of system.

Phase 1: Relay-Assisted Energy Transmission

Let P_{S} denote the transmission power of the source node S. We assume that this power is sufficiently large such that the energy harvested from the noise is negligible. Also, P_{R} and P_{T} are transmission power of relay R and the transmitter T, respectively. In the first phase and first time slot, the transmitter S transmits energy through direct and relay channels. The energy of received signals by the transmitter T and relay R in the first time slot, denoted by superscription (1) in the following equations are

$$E\Big[||y_{\mathrm{T}}^{(1)}||^2\Big] = E\Big[||\sqrt{P_{\mathrm{S}}}h_{\mathrm{ST}}x_{\mathrm{S}}^{(1)} + n_{\mathrm{T}}||^2\Big] \tag{3.6}$$

$$E\Big[||y_{\mathrm{R}}^{(1)}||^2\Big] = E\Big[||\sqrt{P_{\mathrm{S}}}h_{\mathrm{SR}}x_{\mathrm{S}}^{(1)} + n_{\mathrm{R}}||^2\Big] \tag{3.7}$$

respectively, where $E\{.\}$ and $||.||$ denote the expectation and L2-norm operations, $x_{\mathrm{S}}^{(1)}$ is the signal generated from the transmitter S in the first time slot, while n_{R} and n_{T} are the AWGN at relay and the transmitter T, respectively. We assume that we have Binary Phase-Shift Keying (BPSK) modulation at the input signal and as a result $E[||x_{\mathrm{S}}^{(1)}||^2] = 1$.

The relay node is equipped with a harvesting function to harvest received energy during the first time slot using power splitting. We assume that the source S has a fixed energy supply, while a relay has no energy (or is not willing to spend its own energy) to help the source. The relay forwards energy harvested from the source. Let $\alpha \in [0, 1]$ denote the power splitting factor. More specifically, the relay splits a portion of the received energy α for its operation and remaining $(1-\alpha)$ for energy harvesting. The harvested energy at relay will be transferred to the transmitter T. Therefore, noting (1) in [39], the amount of energy harvested by relay R and the transmitter T during the first time slot can be expressed as

$$E_{\mathrm{R}}^{(1)} = (1-\alpha)\eta_{\mathrm{R}}\frac{\tau T}{2}P_{\mathrm{S}}h_{\mathrm{SR}} \tag{3.8}$$

$$E_{\mathrm{T}}^{(1)} = \eta_{\mathrm{T}}\frac{\tau T}{2}P_{\mathrm{S}}h_{\mathrm{ST}} \tag{3.9}$$

where η_{R} and η_{T} are the energy harvesting efficiency at relay and the transmitter nodes. The transmitted relay power is thus given by

$$P_{\mathrm{R}} = \frac{E_{\mathrm{R}}^{(1)}}{\frac{\tau T}{2}} = (1-\alpha)\eta_{\mathrm{R}}P_{\mathrm{S}}h_{\mathrm{SR}} \tag{3.10}$$

Hence, the received energy at the transmitter T by relay R in the second time slot, denoted by superscription (2) in the following equation, can be written as

$$E\Big[||y_{\mathrm{T}}^{(2)}||^2\Big] = E\Big[||\sqrt{P_{\mathrm{R}}}h_{\mathrm{RT}}y_{\mathrm{R}}^{(1)} + n_{\mathrm{T}}||^2\Big] \tag{3.11}$$

In case the received energy at relay R is less than the amount needed for its own operation, relay will not forward any energy to transmitter T, during the first time slot. Since S $\rightarrow$ R power channel is modeled using AWGN channel, energy outage at the node can be written as follows

$$\mathrm{P}_{\mathrm{R}}^{\mathrm{E}} = \text{Prob(outage at relay)} = \mathrm{Prob}(X_{\mathrm{R}}^{(1)} \leq \theta_{\mathrm{R}}) = \int_{-\infty}^{\theta_{\mathrm{R}}} N(\mu_{\mathrm{SR}}, \sigma_{\mathrm{SR}}^2)dx = \frac{1}{2\Big[1 + erf(\frac{\theta_{\mathrm{R}}-\mu_{\mathrm{SR}}}{\sigma_{\mathrm{SR}}\sqrt{2}})\Big]} \tag{3.12}$$

where Pr(.) denotes probability, $X_{\mathrm{R}}^{(1)}$ is a random variable representing received energy at relay node over first time slot, $\mu_{\mathrm{SR}} = 1$, θ_{R} is required energy for relay to operate and $erf(.)$ is the Gaussian error function. According to (3.2), σ_{SR}^2 in this equation depends on Signal to Noise Ratio (SNR) of S $\rightarrow$ R channel which is

$$\gamma_{\mathrm{SR}} = \frac{\alpha \eta_{\mathrm{R}} P_{\mathrm{S}} h_{\mathrm{SR}}}{N_0} \tag{3.13}$$

where N_0 is power spectrum of the white noise and α is the portion of the energy used by relay as defined before. Similarly, SNR of S $\rightarrow$ T and R $\rightarrow$ T channels are

$$\gamma_{\mathrm{ST}} = \frac{\eta_{\mathrm{T}} P_{\mathrm{S}} h_{\mathrm{ST}}}{N_0} \tag{3.14}$$

$$\gamma_{\mathrm{RT}} = \frac{\eta_{\mathrm{T}} P_{\mathrm{R}} h_{\mathrm{RT}}}{N_0} \tag{3.15}$$

where P_{R} is derived in equation (3.10).

If we do not have outage at relay node, in the second phase and the third time slot when the transmitter T attempts to send data to the destination D, the outage probability is defined for the case when the total received energy at the transmitter T through direct and relay links over the first and second time slots is less than the required transmit power threshold θ_{T} at the transmitter. Let $X_{\mathrm{ST}}^{(1)}$, $X_{\mathrm{SR}}^{(1)}$, $X_{\mathrm{RT}}^{(2)}$, $X_{\mathrm{SRT}}^{(1),(2)}$, $X_{\mathrm{T}}^{(1)}$ and $X_{\mathrm{T}}^{(1),(2)}$ denote random variables representing received energy which subscripts and superscripts represent channel names and time slots. Since total energy received at the transmitter T is equal to the sum of energy received by relay and direct links during the first and second time slots, its PDF can be calculated by convolution of direct and relay channels PDFs as follows

$$f_{X_{\mathrm{T}}^{(1),(2)}}(x) = f_{X_{\mathrm{ST}}^{(1)}}(x) * f_{X_{\mathrm{SRT}}^{(1),(2)}}(x) \tag{3.16}$$

For simplicity in two cascaded channels PDF calculations, we assume that S $\rightarrow$ R and R $\rightarrow$ T channels are modeled using AWGN-AWGN channel models, respectively. The PDF of relay channel over the first and second time slots can be calculated as follows

$$f_{X_{\mathrm{SRT}}^{(1),(2)}}(x) = f_{X_{\mathrm{SR}}^{(1)}}(x) * f_{X_{\mathrm{RT}}^{(2)}}(x) = N(\mu_{\mathrm{SRT}}, \sigma_{\mathrm{SRT}}^2) \tag{3.17}$$

where $\mu_{\mathrm{SRT}} = \mu_{\mathrm{SR}} + \mu_{\mathrm{RT}}$, $\sigma^2_{\mathrm{SRT}} = \sigma^2_{\mathrm{SR}} + \sigma^2_{\mathrm{RT}}$ and σ^2_{RT} depends on instantaneous SNR of R $\rightarrow$ T channel which is defined before. For the case when the S $\rightarrow$ T energy channel is modeled using Rician channel model, the PDF of total energy received by the transmitter T resulting from relay and direct links can be calculated using relevant equations calculated before as:

$$f_{X_{\mathrm{T}}^{(1),(2)}}(x) = N(\mu_{\mathrm{SRT}}, \sigma^2_{\mathrm{SRT}}) * h(x, \sigma^2_{\mathrm{ST}}) = \frac{1}{\sqrt{2\pi\sigma^2_{\mathrm{SRT}}}} e^{-(x-\mu_{\mathrm{SRT}})^2/2\sigma^2_{\mathrm{SRT}}} * \left(\frac{x}{\sigma^2_{\mathrm{ST}}} e^{-(x^2+v^2)/2\sigma^2_{\mathrm{ST}}} I_0\left(\frac{xv}{\sigma^2_{\mathrm{ST}}}\right)\right) \tag{3.18}$$

where σ^2_{ST} depends on instantaneous SNR of S $\rightarrow$ T channel which is defined before. Outage probability is the probability that the received energy is less than the energy required to transmit. As a result, the outage probability when relay assists in energy transmission can be calculated using as follows

$$\overset{\triangle}{\mathrm{P}}{}^{\mathrm{E}}_{\mathrm{T}} = \text{Prob(energy outage with relay)} = \text{Prob}(X_{\mathrm{T}}^{(1),(2)} \leq \theta_{\mathrm{T}}) = \int_{-\infty}^{\theta_{\mathrm{T}}} f_{X_{\mathrm{T}}^{(1),(2)}}(x)dx \tag{3.19}$$

where θ_{T} is the minimum required transmit energy at the transmitter T for data transmission. In the special case when there is an outage at relay node, the transmitter T only receives energy from direct channel S $\rightarrow$ T over the first time slot and energy outage probability in this case is

$$\bar{\mathrm{P}}{}^{\mathrm{E}}_{\mathrm{T}} = \text{Prob(energy outage w/o relay)} = \text{Prob}(X_{\mathrm{T}}^{(1)} \leq \theta_{\mathrm{T}}) = \int_{-\infty}^{\theta_{\mathrm{T}}} h(x, \sigma^2_{\mathrm{ST}})dx \tag{3.20}$$

Phase 2: Data Transmission

In the phase 2, the transmitter T transmits data through the direct link to the destination D in the third time slot. The transmitter power is supplied through direct and relay links in the first and second time slots. We assume that the transmitter T has fixed energy for its operation and the total harvested energy over two time slots will be stored in its battery and be used for data transmission in the third time slot. Harvested energy by the transmitter T

over the first and second time slots, can be written as follows

$$E_{\mathrm{T}}^{(1),(2)} = E_{\mathrm{T}}^{(1)} + E_{\mathrm{T}}^{(2)} = \eta_{\mathrm{T}} \frac{\tau T}{2} P_{\mathrm{S}} h_{\mathrm{ST}} + \eta_{\mathrm{T}} \frac{\tau T}{2} P_{\mathrm{R}} h_{\mathrm{RT}} \tag{3.21}$$

As a result, the data transmission power of the transmitter in the relay-assisted scenario where there is no outage at relay node can be expressed as follows

$$P_{\mathrm{T}}^{\text{Relay Assisted}} = \frac{E_{\mathrm{T}}^{(1),(2)}}{(1-\tau)T} \tag{3.22}$$

Thus, the energy of the received signal by the destination D in the third time slot, denoted by superscription (3) in the following equation, can be written as

$$E\Big[||y_{\mathrm{D}}^{(3)}||^2\Big] = E\Big[||\sqrt{P_{\mathrm{T}}} h_{\mathrm{TD}} x_{\mathrm{T}}^{(3)} + n_{\mathrm{D}}||^2\Big] \tag{3.23}$$

where $x_{\mathrm{T}}^{(3)}$ is the signal generated from the transmitter T in the third time slot, while n_{D} is the AWGN at the destination D and P_{T} is the transmission power of the transmitter T.

Data outage happens when the noise on the data channel is more than defined threshold θ_{Data}. For the case when T $\rightarrow$ D data channel is modeled using a Rayleigh channel model, data outage in the relay-assisted scenario can be approximated as follows

$$\mathrm{P}_{\mathrm{T}}^{\mathrm{D}} \overset{\triangle}{=} \text{Prob(data outage with relay)} = \text{Prob}(X_{\mathrm{D}}^{(3)} \leq \theta_{\mathrm{Data}}) = \int_{-\infty}^{\theta_{\mathrm{Data}}} \frac{y}{\sigma_{\mathrm{TD}}^2} e^{-\frac{y}{2\sigma_{\mathrm{TD}}^2}} dy \tag{3.24}$$

where $X_{\mathrm{D}}^{(3)}$ is a random variable representing data received at the destination node D over the third time slot, θ_{Data} is data channel threshold and σ_{TD}^2 depends on SNR of T $\rightarrow$ D channel which is

$$\gamma_{\mathrm{TD}} = \frac{P_{\mathrm{T}}^{\text{Relay Assisted}} h_{\mathrm{TD}}}{N_0} \tag{3.25}$$

and $P_{\mathrm{T}}^{\text{Relay Assisted}}$ is derived in (3.22). In case which there is outage at relay node, data outage in direct energy transmission scenario without having relay $\bar{\mathrm{P}}_{\mathrm{T}}^{\mathrm{D}}$= Pr(data outage w/o relay), can be calculated as following

$$P_{\mathrm{T}}^{\text{Direct}} = \frac{E_{\mathrm{T}}^{(1)}}{(1-\tau)T} \tag{3.26}$$

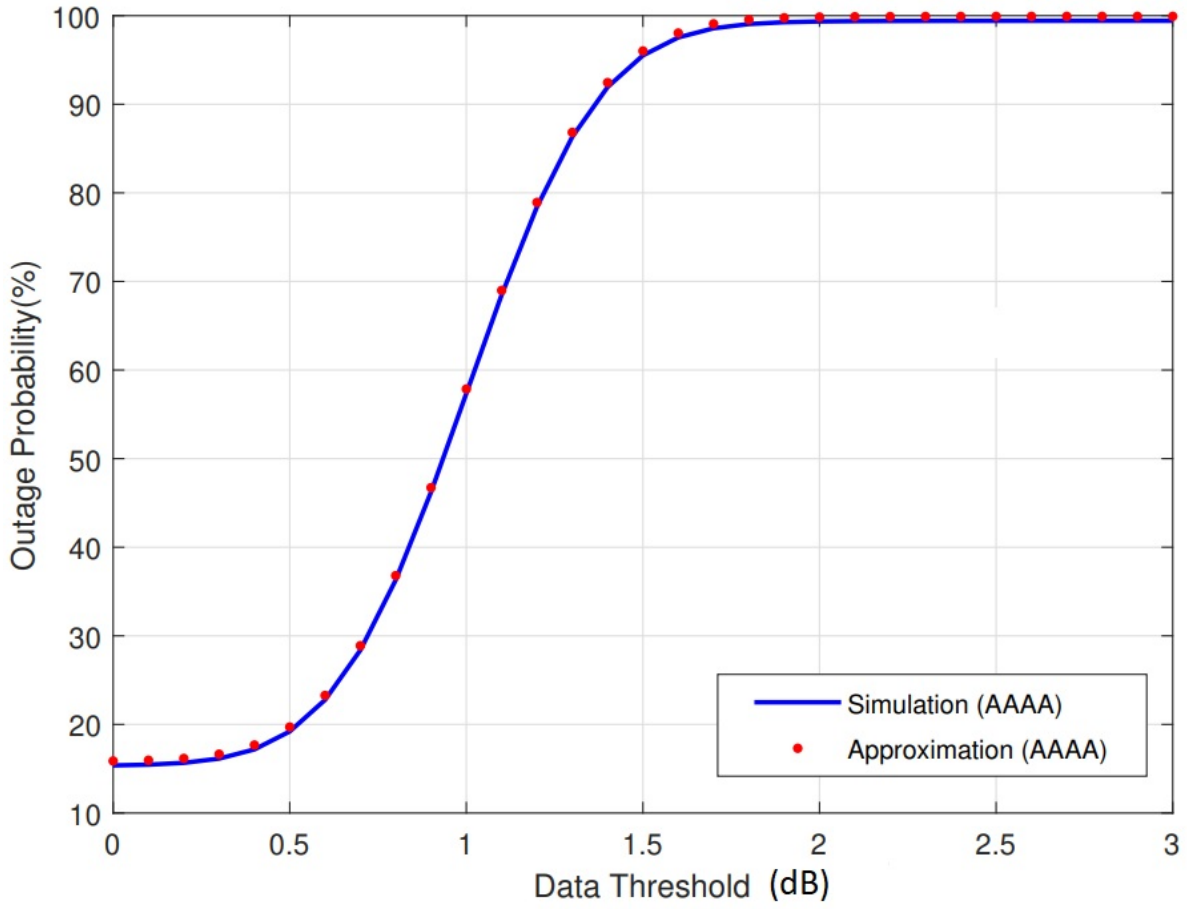

Figure 3.3. Analytically calculated outage vs data threshold verified by simulation for proposed relay-assisted scheme. All channels are modeled using AWGN model denoted by AAAA.

3.5 Simulation Results

Simulations are conducted using MATLAB to verify the analytical calculations for various energy and data channel model combinations using AWGN, Rayleigh, and Rician models. In all simulation figures, the channel names correspond to the S $\rightarrow$ R, R $\rightarrow$ T, S $\rightarrow$ T and T $\rightarrow$ D channels and abbreviations A, R and C indicate AWGN, Rayleigh and Rician channels, respectively.

The outage versus the data threshold with the inclusion of proposed relay-assisted energy transmission scenario is represented in figure 3.3. This figure compares the calculated system

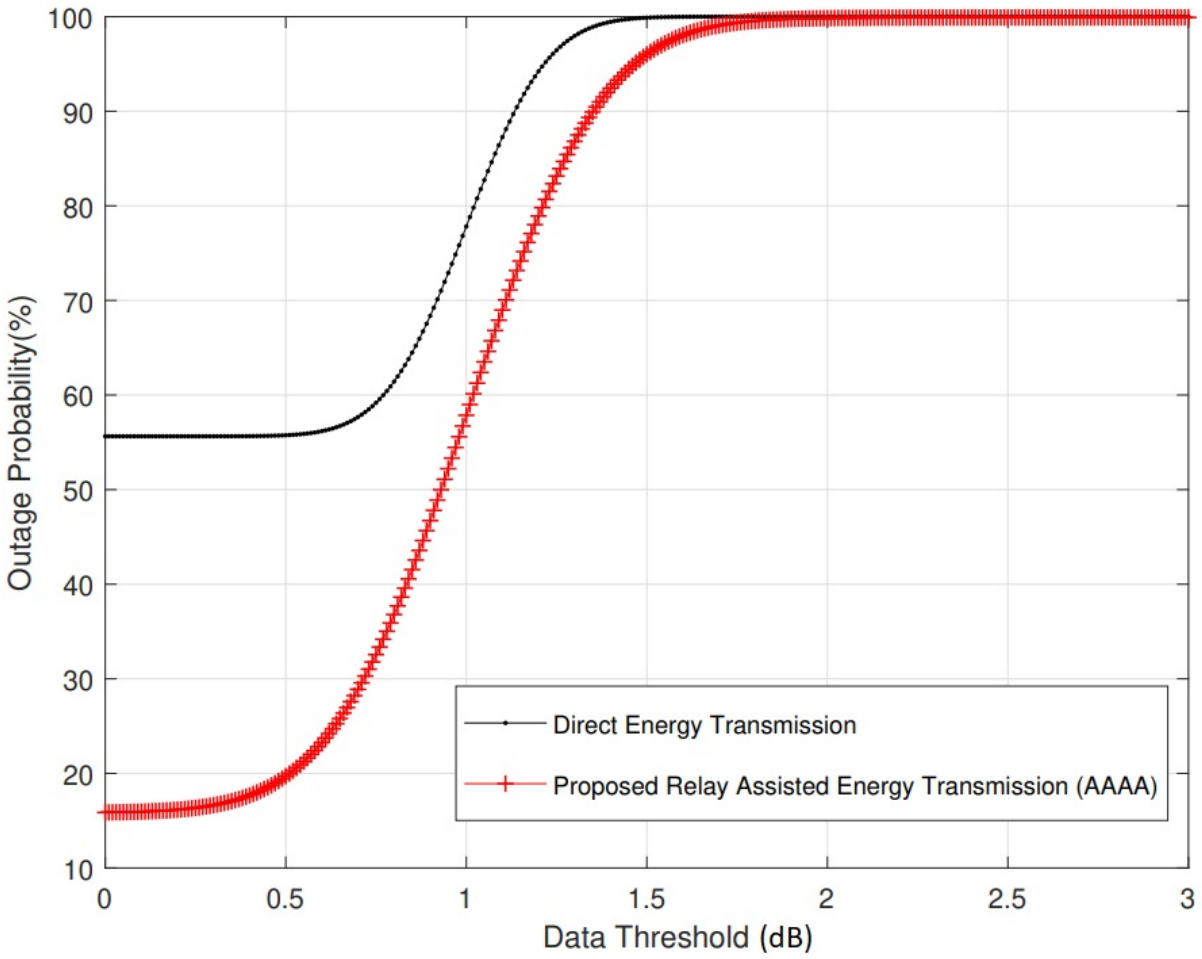

Figure 3.4. Proposed relay-assisted system outage compared to direct energy transmission with no relay for AWGN model for all channels denoted by AAAA.

outage with Monte-Carlo simulations and shows the accuracy of our calculations. The Monte-Carlo method is a novel and flexible approach to multipath channel simulation [93].

When the data threshold is low, the sensor never transmits and therefore never uses energy and it will result in data outage of zero percent and conversely, when the system has a high data threshold the sensor will transmit at every time slot resulting in a maximum data outage probability and consequently system outage probability. For a desired outage level and design criteria, an appropriate threshold may be chosen using this graph. From a practical point of view, it is of value to be able to calculate system outage based on data threshold. It might not be possible to choose the environment the system is in, but we can

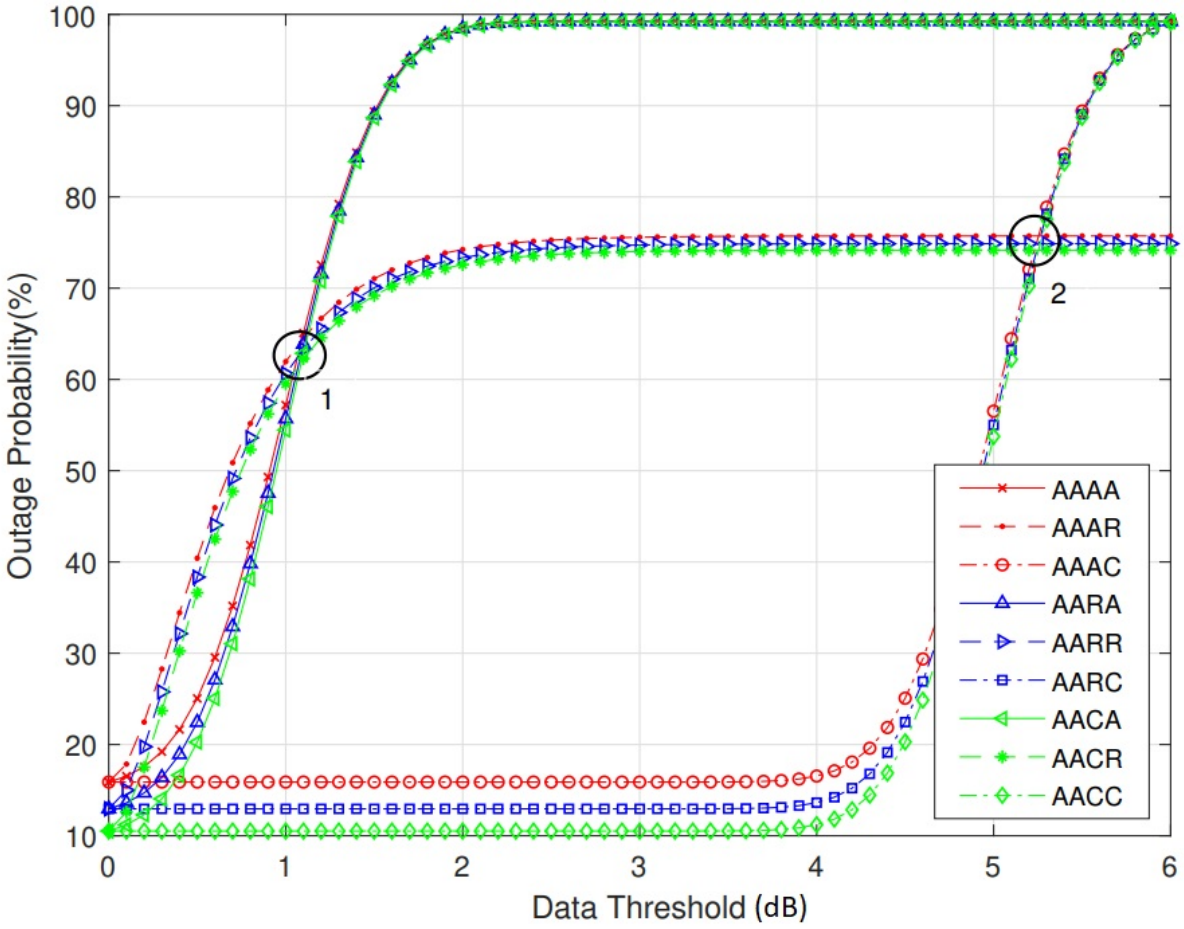

Figure 3.5. System outage probability for various energy and data channels. Channel names correspond to the S → R, R → T, S → T and T → D channels and abbreviations A, R and C indicate AWGN, Rayleigh and Rician channels, respectively.

choose a data threshold to maximize the number of successful transmissions and minimize the outage.

Figure 3.4 compares the outage probability of our proposed relay-assisted energy transmission scenario with the case that there is only energy transmission over the direct link without having any relay versus data threshold. As we can see from this figure, in the proposed relay-assisted scenario the system outage is decreasing significantly which shows the effectiveness of the proposed scheme in this work.

The system outage versus data threshold in all possible channel model combinations is represented in figure 3.5. Channel names correspond to the S → R, R → T, S → T and T →

D channels and abbreviations A, R and C indicate AWGN, Rayleigh and Rician channels, respectively. There are two crossover points at data threshold 1.1 and data threshold 5.3. As we can see, for data thresholds less than first crossover point, the best outage probability performance is for the channel combinations that there are Rician channels and the worst is for Rayleigh channel model at T $\rightarrow$ D. Between the first and second crossover points, the best performance is for Rician and the worst is for AWGN and after second crossover point the best performance is for the Rayleigh and the worst is for the AWGN channel at T $\rightarrow$ D.

3.6 Concluding Remarks

WET technology has recently drawn significant attention since it can solve battery replacement problems of conventional battery powered wireless sensor boards and limited communication range of passive battery free sensors. In this thesis, another dimension of this emerging technology that can significantly impact efficient spectrum sharing is presented. Relay-assisted energy transfer concept combined by intelligent scheduling of transmissions based on available power and channel conditions has been shown to improve our efficiency in accessing spectrum and minimizing power consumption. In this thesis, we proposed and analyzed a relay-assisted energy transmission scenario and modelled data and energy channels, separately. Various static, mobile, highly scattered without and with LOS channel models are all studied. Energy efficient transmission scheduling for the data channel was shown to reduce outage probability, save on power, and minimize unnecessary spectrum access by avoiding transmitting data on a noisy channel or when the transmitter does not have enough power to successfully transmit data. Outage probability of system including sensor energy outage (running out of energy) and data outage and its relationship with a threshold (when to transmit based on channel condition) was derived analytically. In addition, we can see from simulation results that proposed relay-assisted energy transmission scheme can decrease the outage probability of the system. Future research can include study of an scaled up network to develop new methods at the network level and further improving the proposed concept.

The result of this chapter has be published in the following journal and conference:

- S. Naderi, S. Khosroazad, and A. Abedi, "Relay-Assisted Wireless Energy Transfer for Efficient Spectrum Sharing in Harsh Environments," International Journal of Wireless Information Networks (IJWIN), Jan 2022, pp. 1-10.

- S. Naderi, S. Khsroazad, A. Abedi, “From Passive to Active Sensing: Relay-Assisted Wireless Energy Transfer”, 7th IEEE International Conference on Wireless for Space

and Extreme Environments (WiSEE), Passive Wireless Sensor Technology Workshop, Ottawa, ON, Canada, Oct 2019.

CHAPTER 4
OUTAGE PROBABILITY OPTIMIZATION OF SOLAR POWERED CELLULAR BASE STATIONS BASED ON NUMBER OF BATTERIES AND PV PANEL SIZE

4.1 Background

Cellular BSs are important parts of WSN that need to be considered in this thesis. Solar powered BSs are becoming increasingly popular since they are a green solution for network operators and reduce the carbon footprints of such networks. The number of cellular BSs and cellular subscribers has been increasing rapidly which results in higher amounts of energy consumption and the carbon footprint cast by such systems. [44]. There are 43000 solar powered BSs around the globe based on a report in 2014, producing great amounts of energy for cellular networks [45, 46]. Solar powered BSs are very popular since they extend the cellular coverage and decrease the carbon footprint by using renewable energy [47]. These kind of BSs harvest solar energy during the day by using PV panels for their operations. The excess power will be stored in their batteries for their night time operations and bad weather days.

The PV panel size and number of batteries are always the challenging part of designing these BSs since appropriate design results in significant reductions in system cost. Using large panel size and more batteries makes the system more reliable, but alternately, much more expensive. Small panel size and small battery configuration results in greater system outage and lower system reliability. System outage occurs when the BS does not have enough energy for its operation. Frequent system outage causes bad QOS for customers and results in the wasting of resources.

Finding the optimal PV panel size and number of batteries to keep the system outage more than a specific tolerable threshold is a challenging part of designing such a cellular systems. The optimal configuration is a configuration with the least cost that satisfies

operator power outage considerations of the system [47]. In order to solve this problem, outage of the system should be calculated in terms of the PV panel size and number of batteries.

The problem of power outage probability in terms of different system parameters such as BS battery level is considered in recent literature. Battery level at the BS is modeled by discrete time Markov chain and a closed term expression for outage probability is derived for different states in the considered model. Dimensioning guidelines are important aspects of such a system. These are considered in [51, 52, 53, 54, 55, 56, 57, 58]. Authors in [59, 60] used long term solar irradiation data for resource cost optimal dimensioning in cellular BSs. Some literature considered simulation based approaches using commercial software. However these methods are very time consuming from a computation aspects and they do not provide the performance of the system for design purposes [61].

Authors in [62] modeled energy storage in BS with Markov chains and solar irradiation with exponential distributions. Modeling the solar energy in solar powered BSs as a Markov process has been using in great extent in the recent literature [63, 64]. Markov models are used in [65] for modeling solar energy and based on that PV panel size and number of batteries, system configuration is determined in a more accurate, cost optimal approach.

To the best of our knowledge, there is no work that considers the problem of outage probability calculations of solar powered BS in terms of BS load, battery level and harvested solar energy in the U.S. state of Maine. In this last chapter of this thesis, we propose a model for evaluating the outage probability of solar powered BS based on the PV panel size and number of batteries for harvested solar energy by BS in the U.S. state of Maine during different weather conditions and BS load at different days of the week. We evaluate the performance and accuracy of the proposed system in different conditions by simulation and find the required PV panel size and number of batteries for specific tolerable outage probability of the system.

4.2 System model

In this section we present the system model and define parameters. We model BS load, harvested solar energy by PV panels, and battery level. All models are described below in detail.

A. Model for BS Power Consumption and BS Load

In this chapter we consider a Long Term Evolution (LTE) Micro BS. The BS power consumption consists of a fixed part and a variable part; these are modeled as follows [94]:

$$P_{BS} = N_{TRX}(P_0 + \Delta_\rho P_{max}\rho), 0 \leq \rho < 1 \tag{4.1}$$

where P_0 is the power consumption at the BS when there is no traffic, N_{TRX} is the number of transceivers, Δ_ρ is the slope of the load dependent power consumption, P_{max} is the power amplifier output at the maximum traffic, and ρ is the normalized traffic at the given time. Values of P_0, ρ and Δ_ρ for a macro BS are typically considered 118.7W, 40W and 2.66, respectively [94].

As we mentioned, ρ is the normalized traffic at the given time and can be calculated by dividing the number of users at a specific time by the maximum number of BS calls at any time. The traffic is modeled using call based model proposed in [95]. In this model, arrival of the calls are considered as a Poisson process and duration of the call are modeled as exponential distribution with mean of two minutes [96]. The BS load depends on the day of the week. On the weekends, the BS expects to experience less load [97]. Depending on the day of the week, we model the BS load as low (L1) and high (L2) load types. Also we model BS load type as a two state Markov process with transition probability matrix as following:

$$T_L = \begin{bmatrix} q_{11} & q_{12} \\ q_{21} & q_{22} \end{bmatrix} \tag{4.2}$$

where q_{11} is the transition probability from a low load day to a low load day, q_{22} is the transition probability from a high load day to a high load day. Also, $q_{12} = 1 - q_{11}$ is the

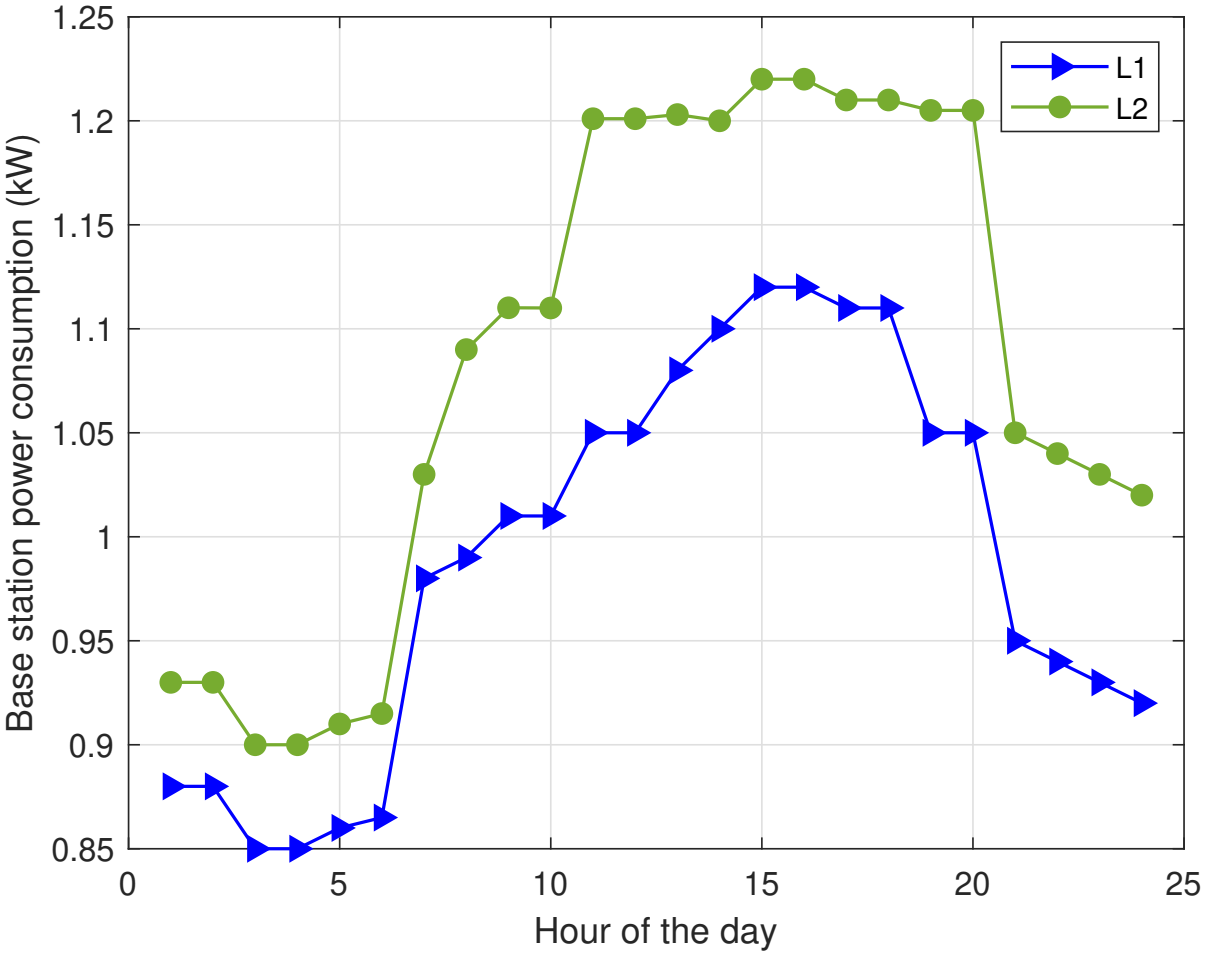

Figure 4.1. Average load profile for a low load and a high load day for the U.S. State of Maine. L1 and L2 refer to low and high load types, respectively.

probability of transition from low load day to a high load day and $q_{21} = 1 - q_{22}$ is the probability of transition from high load day to a low load day. Next, we define the load profile as following:

$$L = (l_1, l_2, ..., l_{24}). \tag{4.3}$$

where l_1 is the first hour of the day average BS load, l_2 is the second hour of the day average BS load and so on. Since we considered two load types, vector L should have two possible values as following:

$$L : L \in \{L_{L1}, L_{L2}\}, \tag{4.4}$$

where L_{L1} is the average load profile vector for a low load day and L_{L2} is the average load profile vector for a high load day. The average load profile for a low load day and a high load day in the State of Maine is shown in figure 4.1 [2].

B. Model for PV Panel Harvested Solar Energy

In this chapter of the thesis, we use Maine state statistical weather data provided by National Renewable Energy Laboratory in [2]. We use 10 years of solar data for Maine. In order to find the hourly energy generated by a specific PV panel, we feed data to the System Advisor Model developed in [98]. We used a PV panel with DC-AC loss factor amount of 0.8 and default tilt values as used in [99]. The overall DC rating PV_w can be calculated as following:

$$PV_w = n_{PV} E_{panel}. \tag{4.5}$$

where n_{PV} is the number of BS PV panels and E_{panel} denotes DC rating of each PV panel. In this thesis, we model the solar energy profile in Maine with a Markov process [100].

We consider the DC rating of a PV panel as 1 KW. After taking the PV panel harvested solar energy, we classify a specific day in two and three categories separately and compare the results in the simulation section. $S1$ is considered for bad weather days when very low solar energy less than α_1 threshold is harvested. When harvested solar energy is between thresholds α_1 and α_2 we consider that day as category $S2$ which this amount of power is still not enough for the BS operation. The rest of the days will be considered as $S3$. In order to calculate the Markov process transition probability from one day type to another day type, we use the statistical data of solar irradiation during a long period of time. This transition probability matrix is as follows:

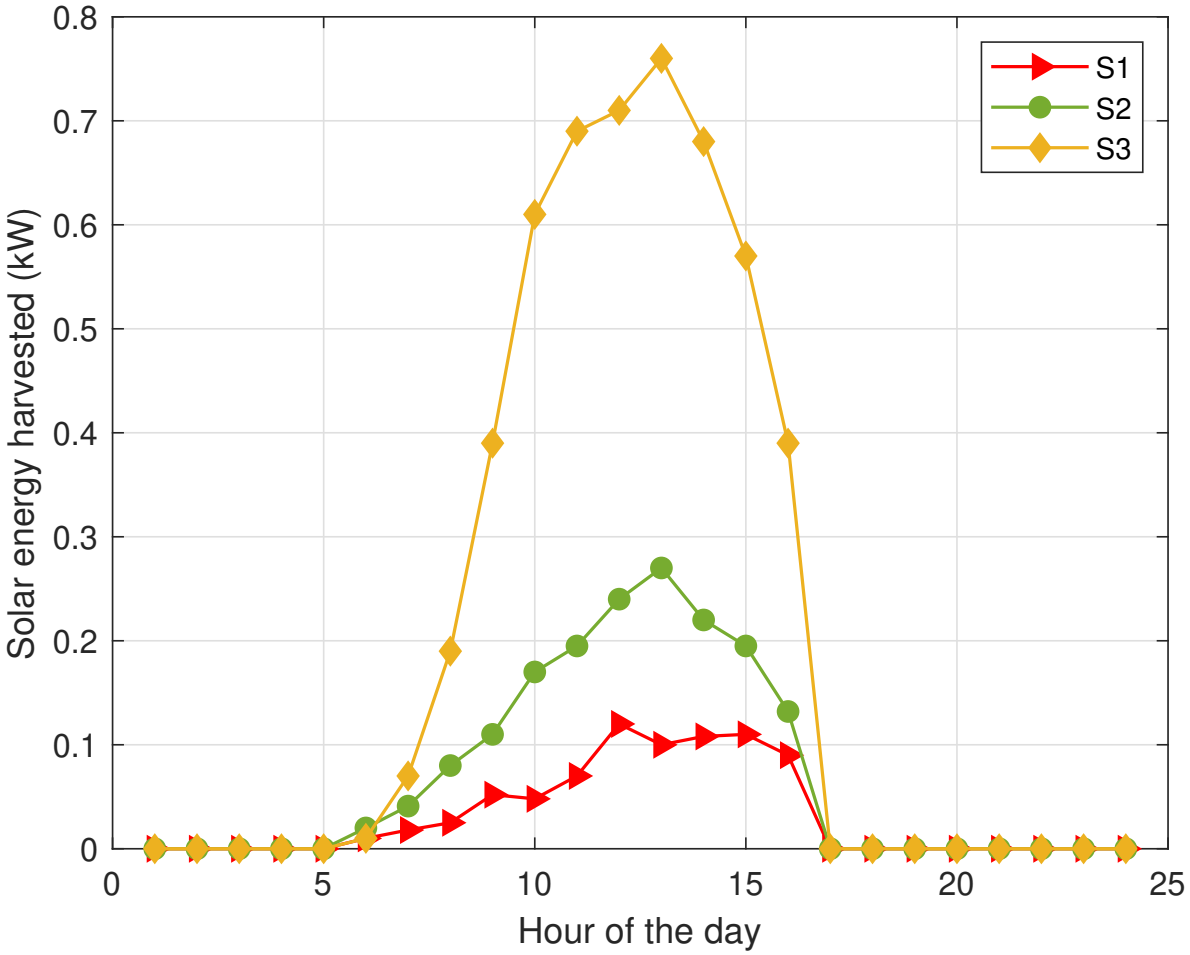

Figure 4.2. Average solar energy harvested for the 3 day types in the U.S. State of Maine [2]. S1 is for days when less than α_1 threshold is harvested. When harvested solar energy is between thresholds α_2 and α_3 we consider that day as category S2. The rest of the days will be considered as S3.

$$T_S = \begin{bmatrix} p_{11} & p_{12} & p_{13} \\ p_{21} & p_{22} & p_{23} \\ p_{31} & p_{32} & p_{33} \end{bmatrix} \tag{4.6}$$

where p_{11} is the probability of a day of type S_1 staying at the same state in the next day and p_{12} is the probability of transition from day type S_1 to day type S_2 next day. The same definition is applied to other variables.

In this chapter, we use the PV panel with 1 KW rating. The average harvested solar energy by the PV panel in each hour of the day can be expressed by the vector S solar energy profile as

$$S = (s_1, s_2, ..., s_{24}). \tag{4.7}$$

where s_1 is the average harvested solar energy in the first hour of the day and so on. As we mentioned before, in this chapter we consider three day types in terms of solar energy harvested and three possible values of vector S are:

$$S : S \in \{S_{s1}, S_{s2}, S_{s3}\}, \tag{4.8}$$

where S_{s1}, S_{s1} and S_{s1} are the profiles for average harvested energy for day types S_1, S_2 and S_3. As shown in figure 4.1, average hourly values of the solar energy harvested in Maine are classified into three day types. As a result, the profile of solar energy harvested by a specific PV panel can be calculated as following:

$$E(t) = PV_w S. \tag{4.9}$$

C. Model for Battery Level

In this thesis, we assume the excess energy harvested by the BS PV panel is stored in the lead acid batteries which are very popular storage options because of their cheaper prices. We assume the BS is using n_b batteries with storage capacities of E_{bat}. As a result the total battery storage capacity can be calculated as following:

$$K_{cap} = n_b E_{bat}. \tag{4.10}$$

In order to model the battery level, first we round total battery storage capacity to the closest integer more than that value and then discretise this value into 1KW blocks. So, the number of battery levels can be calculated as:

$$N = \lceil K_{cap} \rceil. \tag{4.11}$$

At any given point of time, the battery can be in either of the N possible battery levels.

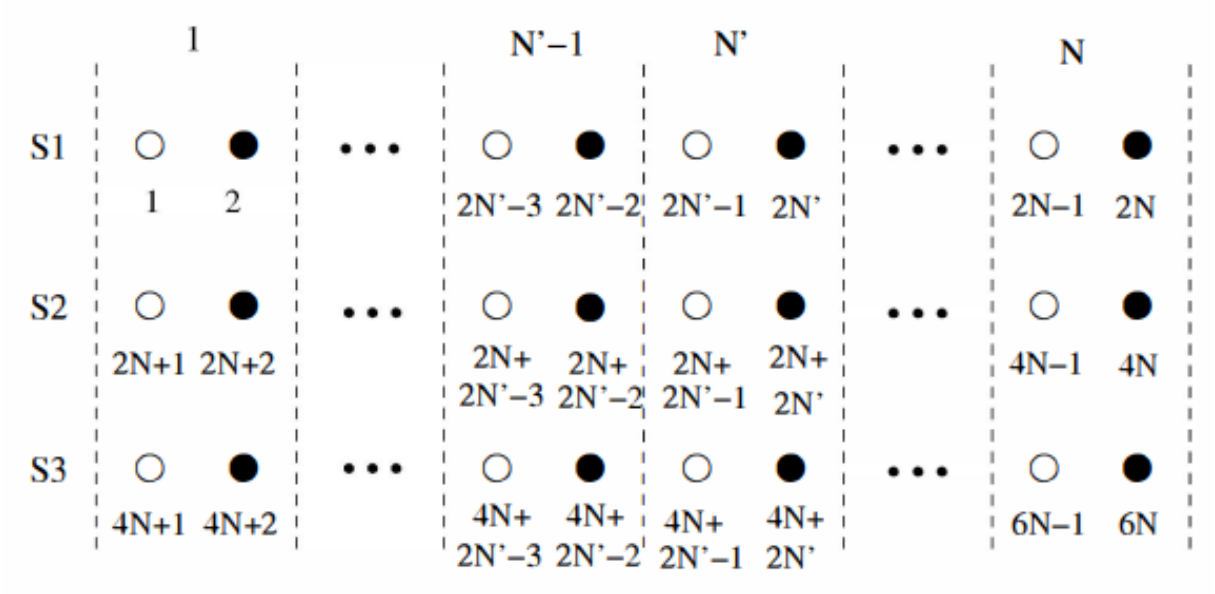

Figure 4.3. System States.

4.3 Base Station Outage Probability Model

We model BS outage in this thesis as the event when the charge level of BS batteries is less than a discharge threshold. The batteries disconnect from the supply bus when they reach their discharge threshold.

As we discussed before, in order to determine the state of the BS in a specific day we need to consider the solar day type, BS load type and battery level. The outage probability of the system can be defined by these three factors. The state of the BS can be defined as:

$$\begin{gathered} i = 2(k-1) + y + 2N(x-1) \\ x \in \{1,2,3\}, y \in \{1,2\}, k \in \{1,2,...,N\} \end{gathered} \tag{4.12}$$

where x is the solar day type for $S1$, $S2$ and $S3$. Also, y is the load type $y = 1$ and $y = 2$ which refer to low load and high load, respectively. In addition, k denotes the battery level. Then the number of possible states are $6N$ since there are three choices for solar day type, N for battery level and two for load type.

All the system possible states are shown in figure 4.3. The first, second and third rows correspond to solar day types $S1$ $(x = 1)$, $S2$ $(x = 2)$ and $S3$ $(x = 3)$, respectively. In each

of the rows the odd positions are showing the low load and even positions showing the high load.

In our model, the state of each day is defined at the beginning of the day and it depends directly to the last days solar energy harvested, load type and battery level. For such a Markov chain the transition probability matrix is:

$$T_B = \begin{bmatrix} b_{(1,1)} & ... & b_{(1,6N)} \\ ... & ... & ... \\ b_{(6N,1)} & ... & b_{(6N,6N)} \end{bmatrix} \tag{4.13}$$

where $b_{(i,j)}$ is the transition probability from state i to state j.

In this thesis, we assume that when the battery charge level goes less than a specific discharge threshold level ν, battery disconnects from the BS. As a result, battery disconnects from BS when its charge level is νK_{cap}. This boundary battery level is as follows:

$$N^{'} = \lceil \nu K_{cap} \rceil \tag{4.14}$$

This battery level $N^{'}$ is also shown in figure 4.4. As a result, the feasible system states are $i \in \{(2N^{'} - 1, 2N) \cup \{(2N^{'} - 1 + 2N, 4N) \cup (2N^{'} - 1 + 4N, 6N)\}$. If we begin a day with a specific amount of solar day type, load type and battery level, the next day's battery level depends on the solar energy and load profiles during the day. The BS outage depends on the battery level, as well. This battery level and consequently outage event is defined in the proposed Algorithm 1 function $F(i)$ in Appendix B.

The function accepts the state of the system i at the beginning of the day as an input and first extract the harvested solar energy, battery level and load profile for the state i. The battery level k is updated, considering the solar energy harvested and load profile variables for every hour during last 24 hour cycle. The limitation for battery level calculation is values between K_{cap} and νK_{cap}. Since only the discrete values are allowed for the battery level, the function rounds the value to the closest integer more than that value. In this model we

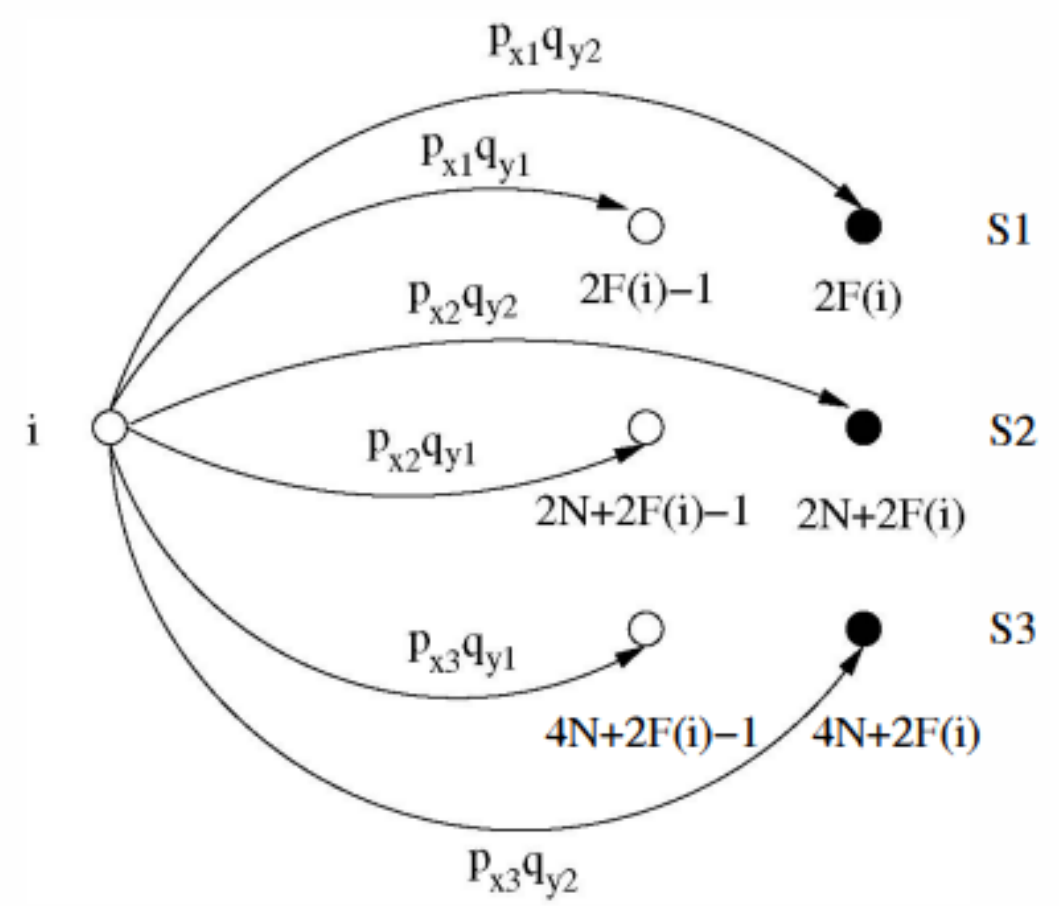

Figure 4.4. Transition graph from state i

record outage events with variable O and use this value for outage calculation at the end. Then, the next battery level in each state i is:

$$k^{'} = F(i) \tag{4.15}$$

Also, the next state can be one state among the six possible states. In each state i, solar day type and load type can be x and y, respectively. All possible state transitions are shown in figure 4.4. The transition probability from state i to state j is:

$$P(i,j) = \begin{cases} p_{x1}q_{y1}, & \text{if } j = 2F(i) - 1, \\ p_{x1}q_{y2}, & \text{if } j = 2F(i), \\ p_{x2}q_{y1}, & \text{if } j = 2F(i) + 2N - 1, \\ p_{x2}q_{y2}, & \text{if } j = 2F(i) + 2N, \\ p_{x3}q_{y1}, & \text{if } j = 2F(i) + 4N - 1, \\ p_{x3}q_{y2}, & \text{if } j = 2F(i) + 4N, \\ 0, & otherwise. \end{cases} \tag{4.16}$$

The transition probability matrix in equation (4.6) can be calculated using equation (4.17). The probability of being in a state π can be calculated as:

$$\pi = \pi T_B \tag{4.17}$$

For each state in vector O, $F(i)$ records the outage status. It stores 1 for outage and 0 for no outage. The outage probability then can be calculated as:

$$\Omega = O.\pi \tag{4.18}$$

For each system configuration, the pv panel (PV_w) and number of batteries (n_b), we can do the similar calculations to compute the outage probability of the system. Considering the outage constraint that is tolerable for a specific configuration is β. We can find the suitable values for PV_w and n_b which satisfies:

$$\Omega \leq \beta \tag{4.19}$$

4.4 System Parameters

In this thesis we use solar irradiance data from NREL. To calculate the generated harvested solar energy by PV panel we use this data as input to the System Advisor Model (SAM) tool [98].

In order to calculate solar energy harvested in a specific month, we consider the solar energy harvested on that month over 10 years. At first, we calculate solar energy harvested on each day and if this value is less than α_1, then we consider that day as type Sl. The harvested energy profile of state S1 in that specific month can be calculated by getting the average of harvested solar energy in each hour of the day type $S1$.

Similarly, we classify the days with harvested solar energy between α_l and α_2 as day type $S2$ and more than α_2 as day type $S3$ and and their harvested energy profile can be calculated in similar way.

This data can be used to find the transition probability matrix for the Markov process corresponding to the daily variations in the solar irradiance in equation (4.6). The same process can be done for threshold α and solar day types $Z1$ and $Z2$.

In order to find the load profiles, we should consider the call arrivals and holding times at BS. The load at BS can be calculated by normalizing these values and using equation (4.1). These are used to find the average hourly values for load profiles of low load days $L1$ and high load days $L2$. The load transition probability matrix of this Markov process in equation (4.2) can then be calculated using these values.

4.5 Simulation Results

In this section, we develop proposed solar powered BS dimension including PV panel size and number of batteries using simulations and find and verify the corresponding outage probability of the system.

A. Simulation setup

We use 2x2 MIMO LTE BS with Bandwidth of 10 MHz. This BS is assumed to have three sectors with two transceivers and then as a result $N_{TRX} = 6$. The batteries used by BS are 12 V, 205 Ah flooded lead acid batteries.

We configure our model for Maine and use solar data from NREL during ten years to find the average harvested solar energy. We assume $\alpha_1 = 1$kW and $\alpha_2 = 2$kW.

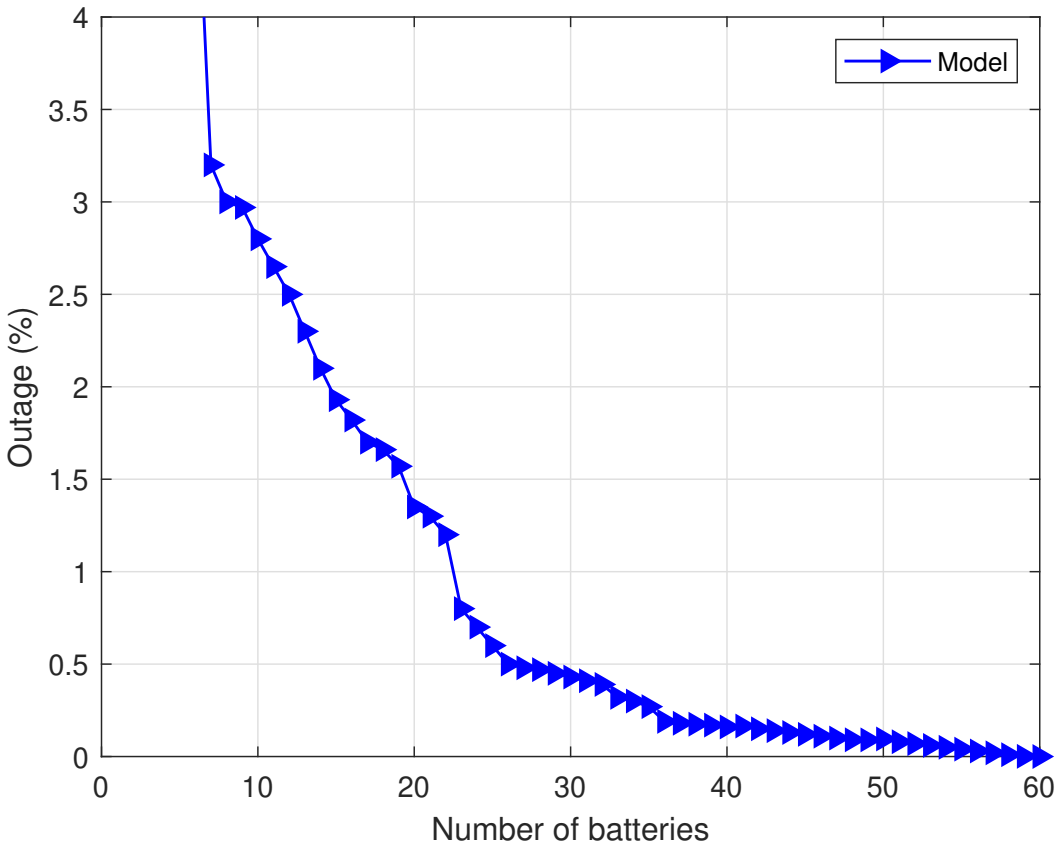

Figure 4.5. Outage vs number of batteries required for PV panel with 12 kW

B. Outage Statistics

First, we study the effect of the number of batteries on outage probability as shown in figure 4.5, assuming PV wattage is 12 kW.

It can be seen from simulation results that the outage probability calculated in our proposed model is increasing very fast for battery sizes less than a specific size. This situation is expected because the batteries are very small to keep enough charge. As a result, we have high amount of outage.

Also, for low outage probability values less than 0.25 very large number of batteries are required. It is obvious that very large number of batteries are needed for BS operation during bad weather days.

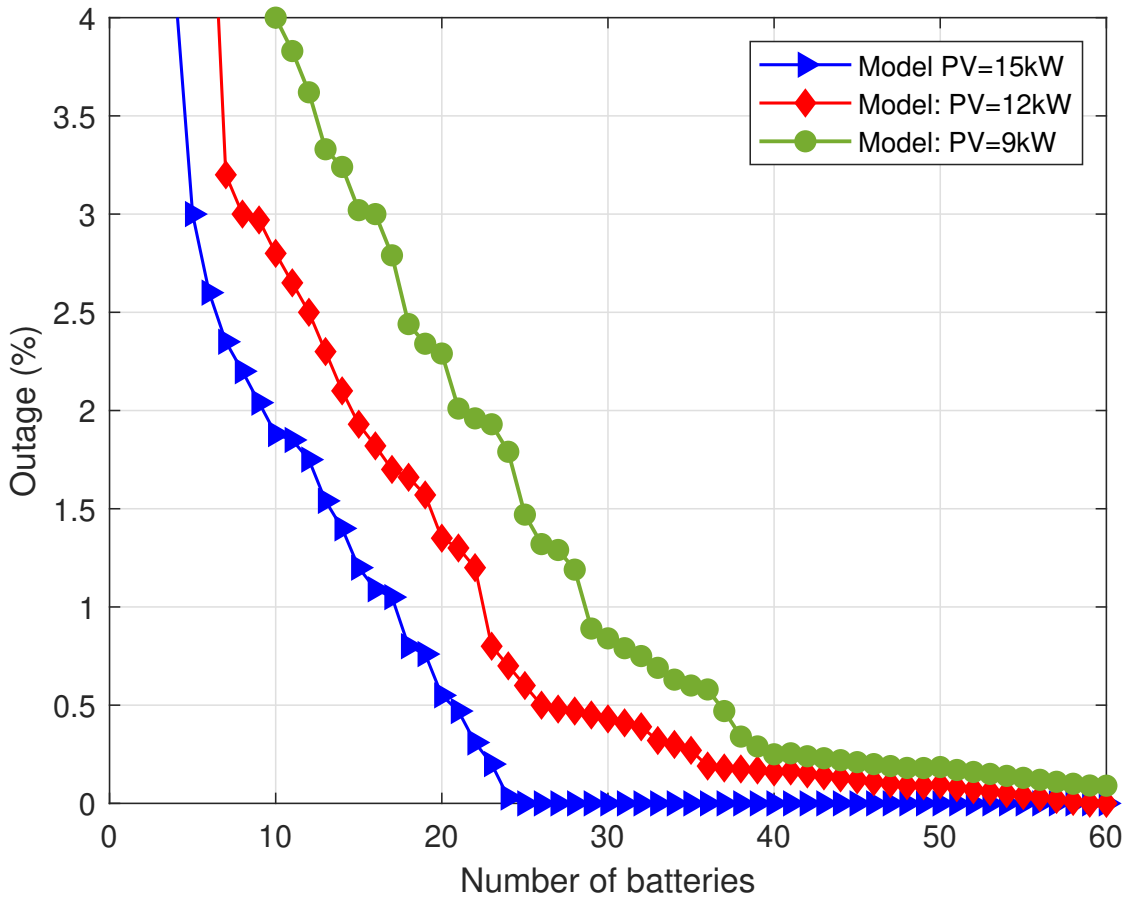

Figure 4.6. Outage vs batteries required for different PV panel sizes

C. Outage Variation with PV Panel Size

Second, we study the effect of PV panel size on the model. We analyze the change in the outage probability of the system for three different PV panel sizes 9 kW, 12 kW and 15 kW with changing in the number of batteries.

The number of required batteries and PV panel size to achieve a specific outage for Maine is shown in figure 4.6. As it can be seen from this figure, by increasing the PV size less, batteries are needed to achieve a specific outage of the system.

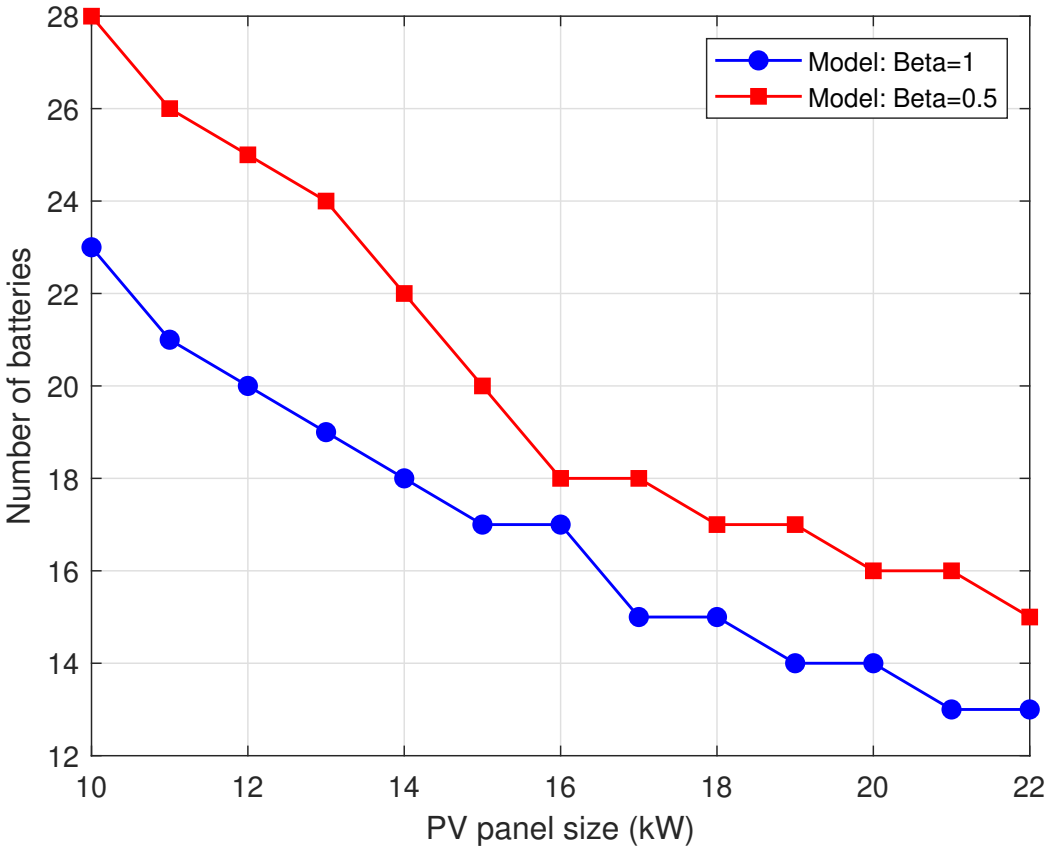

Figure 4.7. Number of batteries vs PV panel size required for different outage probabilities

D. PV Battery Configuration for a Given Outage Constraint

The number of required batteries and PV panel sizes to achieve two tolerable outages $\beta = 0.5$ and $\beta = 1$ is shown in figure 4.7. Using these results the telecom operators can find

the optimum value for PV panel size and number of batteries for a specific tolerable outage probability of the system and find the lowest cost configuration.

4.6 Concluding Remarks

Solar powered cellular BSs are becoming increasingly popular since they are a green solution for network operators and reduce carbon footprints of such a networks. Design of such a system based on the number of batteries and PV panel size for a specific tolerable outage probability with the minimum cost is always a challenging problem.

In this chapter, harvested solar energy, number of batteries and BS load for estimating the outage probability of the solar powered BS is modeled. We proposed a model for evaluating the outage probability of solar powered BS based on the PV panel size and number of batteries for harvested solar energy by BS in Maine during different conditions and BS load at different days of the week. The proposed model is used for Maine solar energy data and the accuracy and effectiveness of the proposed model is verified by simulation results.

Simulation results show the performance of the proposed model and shows the required PV panel size and number of batteries for specific tolerable outage probability of the system.

CHAPTER 5

CONCLUSION

5.1 Summary of Contributions

Forest ecosystem monitoring with high spatio temporal resolution is of paramount importance for development of accurate prediction models. Current systems are bulky, use high power and are costly to build and maintain.

A low cost and reliable wireless soil moisture sensing system is proposed in this thesis to enable data collection for improving our understanding of forest ecosystems. Soil moisture has been increasingly recognized as an important ecosystem property in forested and agricultural systems inspiring the establishment of both soil moisture monitoring networks and large, freely available soil moisture databases.

We have designed a power efficient soil moisture system that is low cost to enable large scale monitoring. The developed methods allow for implementation of low-power sensor networks. We also compared the proposed system with industry standard wired systems in a field experiment. The results show reasonably similar data at much lower cost. This system is power efficient and low cost to enable wide spread monitoring.

Next in this thesis, we considered the problem of spectrum and power efficiency in WSN. Spectrum and energy efficient WSN cooperative model and scheduling method is proposed.

Wireless energy transfer technology has recently drawn significant attention since it can solve battery replacement problem of conventional battery powered wireless sensor boards and limited communication range of passive battery free sensors. In this thesis, another dimension of this emerging technology that can significantly impact efficient spectrum sharing is presented. Relay-assisted energy transfer concept combined by intelligent scheduling of transmissions based on available power and channel conditions has been shown to improve our efficiency in accessing spectrum and minimizing power consumption.

We proposed and analyzed a relay-assisted energy transmission scenario and modelled data and energy channels, separately. Various static, mobile, highly scattered without and with LOS channel models are all studied. Energy efficient transmission scheduling for the data channel was shown to reduce outage probability, save on power, and minimize unnecessary spectrum access by avoiding transmitting data on a noisy channel or when the transmitter does not have enough power to successfully transmit data.

Outage probability of system including sensor energy outage and data outage and its relationship with a threshold was derived analytically and verified by simulations. In addition, we can see from simulation results that the proposed relay-assisted energy transmission scheme can decrease the outage probability of the system.

In the last chapter of this thesis, we analyzed the performance of cellular BSs in WSN. Cellular BSs are important parts of WSN that needed to be considered in this thesis. These types of BSs are becoming increasingly popular since they are a green solution for network operators and reduce carbon footprints of such a networks. The number of cellular BSs and cellular subscribers has been increasing rapidly which results in high amount of energy consumption and carbon footprint cased by such a systems.

The PV panel size and number of batteries are always the challenging part of designing these BSs because appropriate design results in significant decreases in system cost. Using large panel size and and more batteries makes the system of course more reliable but on the other side much more expensive. The small panel size and less batteries results in more system outage and less system reliability as well. System outage occurs when BS does not have enough energy for its operation. Frequent system outage causes bad QOS for customers and results in wasting of resources. Finding the optimal PV panel size and number of batteries to keep the system outage more than a specific tolerable threshold is a challenging part of designing such a cellular systems. The optimal configuration is a configuration with the least cost that satisfies operator power outage considerations of the system. In order to

solve this problem, outage of the system should be calculated in terms of the PV panel size and number of batteries.

In the last chapter of this thesis we proposed a model for evaluating the outage probability of the solar powered BS based on the PV panel size and number of batteries for harvested solar energy by BS in Maine during different weather conditions in different seasons of the year and BS load at different days of the week.

We calculated the outage probability of the proposed model and evaluated the performance and accuracy of the proposed system in different conditions by simulation. This permitted the discovery of the required PV panel size and number of batteries for specific tolerable outage probability of the system.

5.2 Future Work

Future work on chapter 2 includes enhancing the sensor node with additional sensor types (soil and ambient temperature, snow depth, and more) and scaling up the network with more sensor nodes. Future designs will implement a more efficient and compact antenna, while providing additional range should it be required.

Also, one can be more focused on network level of research including subsystems and metrics.

Subsystem research includes study on nodes (different types, small, large, sensor, relay, processor, etc.), links (short, long, single link, multi link, wired, wireless, etc.) and fusion center (centralized processing/storage, distributed processing/ storage).

For metrics, more focus will be on cost (nodes, various alternative types, assembly, programming, maintenance, life), reliability (probability of failure at node and network level, MTBF, MTTR) and performance (theoretical, experimental, throughput, latency, power needs, etc.).

As shown in figure 5.1, reliability versus power consumption will be considered, for systems with an increased number of sensors and no power amplifier RF output stage.

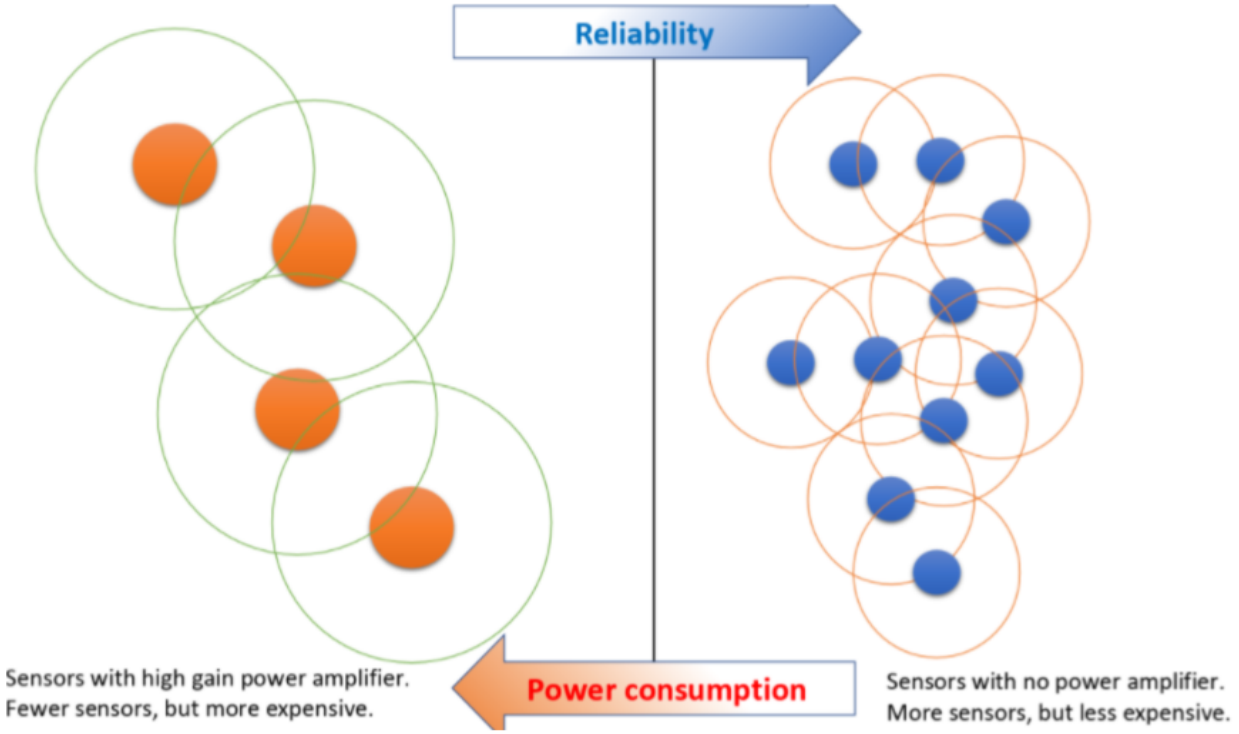

Figure 5.1. Reliability versus power consumption by adding more sensors with no power amplifier Reliability versus power consumption by adding more sensors with no power amplifier.

We expect that when we have fewer more expensive sensors with high gain power amplifier we have less reliability and more power consumption compared to the case where we have more less expensive sensors with no amplifier.

Figure 5.2 proves that reliability be increased by adding more sensors. Sensors with amplifiers exhibit lower reliability in contrast to sensors that do not have amplifiers.

Future research on chapter 3 may include a study of an scaled up network to develop new methods at the network level and further improve the proposed concept.

Proposed work on chapter 4 of this thesis can be expanded by considering more thresholds for harvested solar energy and comparing the accuracy of the system with the current system and finding the optimal number of thresholds for the tolerable outage of the system.

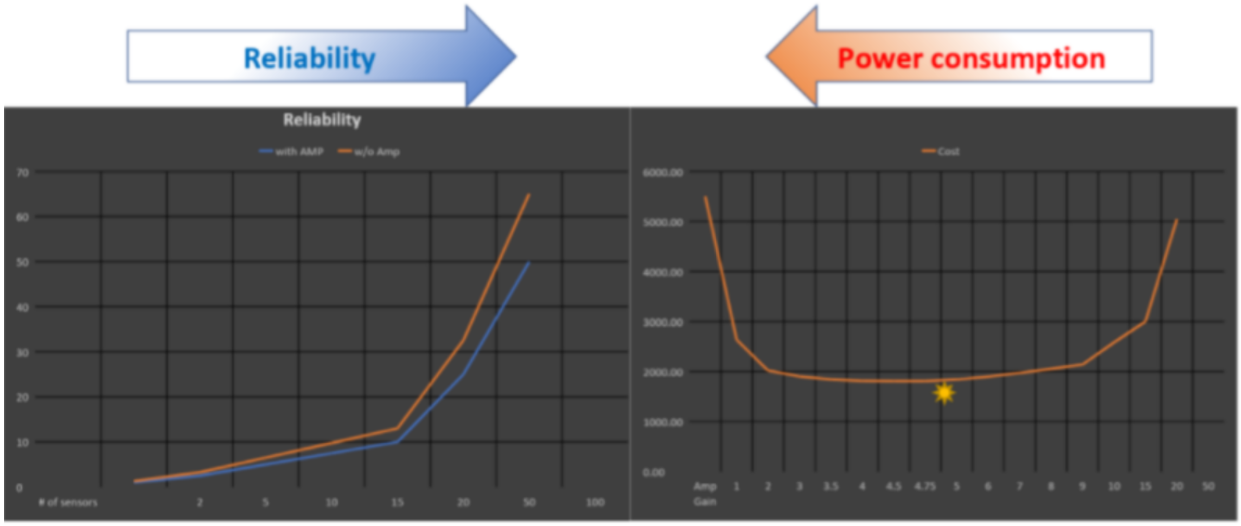

Figure 5.2. Reliability and power consumption curves Reliability and power consumption curves.

5.3 Publications

The results of the research and proposed systems in this thesis have been published and submitted for publication in the following papers.

[1] Outage Probability Optimization of Solar Powered Cellular Base Stations Based on Number of Batteries and PV Panel Size," To be submitted to Springer International Journal of Wireless Information Networks (IJWIN), September 2022.

[2] S. Naderi, K. Bundy, T. Whitney, A. Abedi, A. Weiskittel, and A. Contosta, "Sharing Wireless Spectrum in the Forest Ecosystems Using Artificial Intelligence and Machine Learning," International Journal of Wireless Information Networks (IJWIN), Aug 2022, pp. 1-12.

[3] S. Naderi, S. Khosroazad, and A. Abedi, "Relay-Assisted Wireless Energy Transfer for Efficient Spectrum Sharing in Harsh Environments," International Journal of Wireless Information Networks (IJWIN), Jan 2022, pp. 1-10.

[4] T. Whitney, T. Nicholas, S. Naderi and A. Abedi, "A Low Cost Power Efficient Wireless Soil Moisture Sensor Network for Forest Ecosystem Monitoring," 2020 IEEE MIT Undergraduate Research Technology Conference (URTC), Oct 2020, pp. 1-4.

[5] S. Khosroazad, S. Naderi and A. Abedi, "Using Physical Layer Network Coding to Improve NOMA System Throughput with Energy Harvesting Users," 2019 IEEE Global Communications Conference (GLOBECOM), Waikoloa, HI, USA, 2019, pp. 1-6.

[6] S. Naderi, S. Khsroazad, A. Abedi, “From Passive to Active Sensing: Relay-Assisted Wireless Energy Transfer”, 7th IEEE International Conference on Wireless for Space and Extreme Environments (WiSEE), Passive Wireless Sensor Technology Workshop, Ottawa, ON, Canada, Oct 2019.

REFERENCES

[1] R. Wallace, "Cc-antenna-dk2 and antenna measurements summary."

[2] in *http://www.nrel.gov/rredc/solar$_d$ata.html*, *Lastaccessed* : 2022.

[3] R. K. Dwivedi, S. Pandey, and R. Kumar, "A study on machine learning approaches for outlier detection in wireless sensor network," in *2018 8th International Conference on Cloud Computing, Data Science & Engineering (Confluence)*, 2018, pp. 189–192.

[4] S. Khosroazad, S. Naderi, and A. Abedi, "Using physical layer network coding to improve noma system throughput with energy harvesting users," in *2019 IEEE Global Communications Conference*, 2019, pp. 1–6.

[5] W. Z. Guo, L. J. Hao, and W. J. Di, "Application and development of artificial intelligence technology for the data management and analysis in forestry," in *2009 International Conference on Artificial Intelligence and Computational Intelligence*, vol. 4, 2009, pp. 438–441.

[6] S. I. Seneviratne, T. Corti, E. L. Davin, M. Hirschi, E. B. Jaeger, I. Lehner, B. Orlowsky, and A. J. Teuling, "Investigating soil moisture–climate interactions in a changing climate: A review," in *Earth-Science Reviews*, vol. 99, no. 3-4, 2010, pp. 125–161.

[7] R. D. Koster, P. A. Dirmeyer, Z. Guo, G. Bonan, E. Chan, P. Cox, C. Gordon, S. Kanae, E. Kowalczyk, D. Lawrence *et al.*, "Regions of strong coupling between soil moisture and precipitation," in *American Association for the Advancement of Science*, vol. 305, no. 5687, 2004, pp. 1138–1140.

[8] D. R. Legates, R. Mahmood, D. F. Levia, T. L. DeLiberty, S. M. Quiring, C. Houser, and F. E. Nelson, "Soil moisture: A central and unifying theme in physical geography," in *Progress in Physical Geography, Sage Publications Sage UK: London, England*, vol. 35, no. 1, 2011, pp. 65–86.

[9] J. K. Green, S. I. Seneviratne, A. M. Berg, K. L. Findell, S. Hagemann, D. M. Lawrence, and P. Gentine, "Large influence of soil moisture on long-term terrestrial carbon uptake," in *Nature Publishing Group*, vol. 565, no. 7740, 2019, pp. 476–479.

[10] J. Gornall, R. Betts, E. Burke, R. Clark, J. Camp, K. Willett, and A. Wiltshire, "Implications of climate change for agricultural productivity in the early twenty-first century," in *Philosophical Transactions of the Royal Society B: Biological Sciences*, vol. 365, no. 1554, 2010, pp. 2973–2989.

[11] S. of the art in large-scale soil moisture monitoring, "State of the art in large-scale soil moisture monitoring," in *Soil Science Society of America Journal*, 2013, pp. 1–32.

[12] t. y. v. n.-p. d. Schaefer, Garry L and Cosh, Michael H and Jackson, Thomas J, booktitle=.

[13] t. y. v. n.-p. d. Bell, Jesse E and Palecki, Michael A and Baker, C Bruce and Collins, William G and Lawrimore, Jay H and Leeper, Ronald D and Hall, Mark E and Kochendorfer, John and Meyers, Tilden P and Wilson, Tim and others, booktitle=Journal of Hydrometeorology.

[14] W. Dorigo, W. Wagner, R. Hohensinn, S. Hahn, C. Paulik, A. Xaver, A. Gruber, M. Drusch, S. Mecklenburg, P. v. Oevelen *et al.*, "The international soil moisture network: a data hosting facility for global in situ soil moisture measurements," in *Hydrology and Earth System Sciences*, vol. 15, no. 5, 2011, pp. 1675–1698.

[15] T. Whitney, V. Nicholas, S. Naderi, and A. Abedi, "A low cost power efficient wireless soil moisture sensor network for forest ecosystem monitoring," in *2020 IEEE MIT URTC*. IEEE, 2020.

[16] S. Naderi, K. Bundy, T. Whitney, A. Abedi, A. Weiskittel, and A. Contosta, "Sharing wireless spectrum in the forest ecosystems using artificial intelligence and machine learning," in *International Journal of Wireless Information Networks (IJWIN)*. IEEE, 2022, pp. 1–12.

[17] N. B. A. Karim and I. B. Ismail, "Soil moisture detection using electrical capacitance tomography (ect) sensor," in *2011 IEEE International Conference on Imaging Systems and Techniques*, 2011, pp. 83–88.

[18] S. Bi, C. K. Ho, and R. Zhang, "Wireless powered communication: Opportunities and challenges," in *IEEE Communications Magazine*, vol. 53, no. 4. IEEE, 2015, pp. 117–125.

[19] K. Huang and E. Larsson, "Simultaneous information and power transfer for broadband wireless systems," in *IEEE Transactions on Signal Processing*, vol. 61, no. 23. IEEE, 2013, pp. 5972–5986.

[20] J. Gozalvez, "Witricity-the wireless power transfer [mobile radio]," in *IEEE Vehicular Technology Magazine*, vol. 2, no. 2. IEEE, 2007, pp. 38–44.

[21] R. J. Vyas, B. B. Cook, Y. Kawahara, and M. M. Tentzeris, "E-wehp: A batteryless embedded sensor-platform wirelessly powered from ambient digital-tv signals," in *IEEE Transactions on Microwave Theory and Techniques*, vol. 61, no. 6. IEEE, 2013, pp. 2491–2505.

[22] Z. Popovic, "Cut the cord: Low-power far-field wireless powering," in *IEEE Microwave Magazine*, vol. 14, no. 2. IEEE, 2013, pp. 55–62.

[23] S. Naderi, D. B. da Costa, and H. Arslan, "Joint random subcarrier selection and channel-based artificial signal design aided PLS," in *IEEE Wireless Communications Letters*, vol. 9, no. 7, 2020, pp. 976–980.

[24] S. Naderi, D. B. d. Costa, and H. Arslan, "Channel randomness-based adaptive cyclic prefix selection for secure OFDM system," in *IEEE Wireless Communications Letters*, vol. 11, no. 6, 2022, pp. 1220–1224.

[25] H. Salman, S. Naderi, and H. Arslan, "Channel-dependent code allocation for downlink MC-CDMA system aided physical layer security," in *2022 IEEE 95th Vehicular Technology Conference: (VTC2022-Spring)*, 2022, pp. 1–5.

[26] O. Ozel, K. Tutuncuoglu, S. Ulukus, and A. Yener, "Fundamental limits of energy harvesting communications," in *IEEE Communications Magazine*, vol. 53, no. 4. IEEE, 2015, pp. 126–132.

[27] M. Agiwal, A. Roy, and N. Saxena, "Next generation 5G wireless networks: A comprehensive survey," in *IEEE Communications Surveys & Tutorials*, vol. 18, no. 3. IEEE, 2016, pp. 1617–1655.

[28] D. Liu, L. Wang, Y. Chen, M. Elkashlan, and K.-K. Wong, "User association in 5g networks: A survey and an outlook."

[29] S. Ulukus, A. Yener, E. Erkip, O. Simeone, M. Zorzi, P. Grover, and K. Huang, "Energy harvesting wireless communications: A review of recent advances," in *IEEE Journal on Selected Areas in Communications*, vol. 33, no. 3. IEEE, 2015, pp. 360–381.

[30] B. Gurakan, O. Ozel, J. Yang, and S. Ulukus, "Energy cooperation in energy harvesting wireless communications," in *2012 IEEE international symposium on information theory proceedings*. IEEE, 2012, pp. 965–969.

[31] S. Naderi and M. R. Javan, "Performance analysis of the link selection for secure device-to-device communications with an untrusted relay," in *Turkish Journal of Electrical Engineering & Computer Sciences*, vol. 25, no. 5. The Scientific and Technological Research Council of Turkey, 2017, pp. 3787–3797.

[32] Z. Chen, L. X. Cai, Y. Cheng, and H. Shan, "Sustainable cooperative communication in wireless powered networks with energy harvesting relay," in *IEEE Transactions on Wireless Communications*, vol. 16, no. 12. IEEE, 2017, pp. 8175–8189.

[33] S. Naderi, M. R. Javan, and A. Aref, "Secrecy outage analysis of cooperative amplify and forward relaying in device to device communications," in *2016 24th Iranian conference on electrical Engineering (ICEE)*. IEEE, 2016, pp. 40–44.

[34] A. Aref, S. Naderi, and O. R. Ma'Rouzi, "On the performance evaluation of hybrid decode-amplify-forward relaying protocol with adaptive m-qam modulation over rayleigh fading channels," in *2015 2nd International Conference on Knowledge-Based Engineering and Innovation (KBEI)*. IEEE, 2015, pp. 521–525.

[35] T. Li, P. Fan, and K. B. Letaief, "Outage probability of energy harvesting relay-aided cooperative networks over rayleigh fading channel," in *IEEE Transactions on Vehicular Technology*, vol. 65, no. 2. IEEE, 2015, pp. 972–978.

[36] A. K. Dutta, K. Hari, C. R. Murthy, N. B. Mehta, and L. Hanzo, "Minimum error probability mimo-aided relaying: multihop, parallel, and cognitive designs," in *IEEE Transactions on Vehicular Technology*, vol. 66, no. 6. IEEE, 2016, pp. 5435–5440.

[37] Y. Chen, "Energy-harvesting af relaying in the presence of interference and nakagami-m fading," in *IEEE Transactions on Wireless Communications*, vol. 15, no. 2. IEEE, 2015, pp. 1008–1017.

[38] Z. Ding, S. M. Perlaza, I. Esnaola, and H. V. Poor, "Power allocation strategies in energy harvesting wireless cooperative networks," in *IEEE Transactions on Wireless Communications*, vol. 13, no. 2. IEEE, 2014, pp. 846–860.

[39] H. Chen, Y. Li, J. L. Rebelatto, B. F. Uchoa-Filho, and B. Vucetic, "Harvest-then-cooperate: Wireless-powered cooperative communications," in *IEEE Transactions on Signal Processing*, vol. 63, no. 7. IEEE, 2015, pp. 1700–1711.

[40] S. Veilleux, K. Bundy, A. Almaghasilah, and A. Abedi, "Transmission scheduling for wireless energy transfer with dual data-energy channel models," in *2018 6th IEEE International Conference on Wireless for Space and Extreme Environments (WiSEE)*. IEEE, 2018, pp. 30–35.

[41] S. Naderi, S. Khosroazad, and A. Abedi, "Relay-assisted wireless energy transfer for efficient spectrum sharing in harsh environments," in *International Journal of Wireless Information Networks*. IEEE, 2022, pp. 1–10.

[42] "Mobile marvels." The Economist, 2009.

[43] S. Asif, "Next generation mobile communications ecosystem: Technology management for mobile." Wiley, 2011.

[44] H. Bogucka and O. Holland, "Multi-layer approach to future green mobile communications," in *IEEE Intelligent Transportation Systems Magazine*, vol. 5, no. 4, 2013, pp. 28–37.

[45] "Global system mobile association (gsma), accessed on nov. 5," in *[Online]. Available: http://www.gsma.com/*, 2015.

[46] M. M. and et al., "Optimal energy savings in cellular access networks," in *Proc. IEEE ICC Dresden, Germany*, 2009.

[47] M. M. et. al, "Towards zero grid electricity networking: Powering BSs with renewable energy sources," in *Proc. IEEE ICC, Budapest, Hungary*, 2013.

[48] A. D. C. M. M. M. Marsan, G. Bucalo and Y. Zhang, "Towards zero grid electricity networking: Powering bss with renewable energy sources," in *Proc. IEEE ICC*, Budapest, Hungary, June 2013.

[49] V. B. H. Geirbo and K. Braa, "Leveraging mobile network infrastructure for rural electrification - experiences from an ongoing pilot project in Bangladesh," in *Pro. MILEN, Oslo, Norway*, Norway, November 2012.

[50] N. F. et al., "Powering cell sites for mobile cellular systems using solar power," in *International Journal of Engineering and Technology*, vol. 2, no. 5, 2012, pp. 732–741.

[51] L. B. and G. Oberg, "Solar power for radio base station (RBS) sites applications including system dimensioning, cell planning and operation," in *Proc. 23rd IEEE INTELEC, Edinburgh, U.K.*, 2001, pp. 587–590.

[52] G. P. et al., "Hetnets powered by renewable energy sources: Sustainable next-generation cellular networks," in *IEEE Internet Comput.*, vol. 17, no. 1, 2013, pp. 32–39.

[53] E. Ofry and A. Braunstein, "The loss of power supply probability as a technique for designing stand-alone solar electrical (photovoltaic) systems," in *IEEE Trans. Power App. System*, vol. 102, no. 5, 1983, pp. 1171–1175.

[54] M. M. H. Bhuiyan and M. A. Asgar, "Sizing of a stand-alone photovoltaic power system at dhaka," in *Renew. Energy*, vol. 28, no. 6, 2003, pp. 929–938.

[55] C. Venu, Y. Riffonneau, S. Bacha, and Y. Baghzouz, "Battery storage system sizing in distribution feeders with distributed photovoltaic systems," in *in Proc. IEEE PowerTech, Bucharest, Romania*, 2009, pp. 1–5.

[56] N. F. et al., "Powering cell sites for mobile cellular systems using solar power," in *Int. J. Eng. Technol.*, vol. 2, no. 5, 2012, pp. 732–741.

[57] D. Marquet, O. Foucault, and M. Aubree, "Sollan-dimsol R D project, solar and renewable energy in france telecom„" in *in Proc. 28th IEEE INTELEC, Providence, RI, USA*. 2006, pp. 1–8.

[58] D. Marquet, M. Aubrée, S. Le Masson, A. Ringnet, P. Mesguich, and M. Kirtz, "The first thousand optimized solar BTS stations of orange group," in *in Proc. IEEE 33rd INTELEC, Amsterdam, The Netherlands*, 2011, pp. 1–9.

[59] A. J. et al., "Powering cellular base stations: A quantitative analysis of energy options," in *Department Telecom Center Excellence, Indian Institute Technology*, 2012.

[60] P. Nema, R. K. Nema, and S. Rangnekar, "PV-solar/wind hybrid energy system for GSM/CDMA type mobile telephony base station," in *Int. J. Energy Environ.*, vol. 1, no. 2, 2010, pp. 359–366.

[61] L. Bernal-Agustín and R. Dufo-López, "Simulation and optimization of stand-alone hybrid renewable energy systems," in *Renew. Sustain. Energy Rev.*, vol. 13, no. 8, 2009, pp. 2111–2118.

[62] J. Song, V. Krishnamurthy, A. Kwasinski, and R. Sharma, "Development of a markov-chain-based energy storage model for power supply availability assessment of photovoltaic generation plants," in *IEEE Trans. Sustain. Energy*, vol. 4, no. 2, 2013, pp. 491–500.

[63] H. A. M. Maghraby, M. H. Shwehdi, and G. K. Al-Bassam, "Probabilistic assessment of photovoltaic (PV) generation systems," in *IEEE Trans. Power Syst.*, vol. 17, no. 1, 2002, pp. 205–208.

[64] N. Kakimoto, S. Matsumura, K. Kobayashi, and M. Shoji, "Two-state Markov model of solar radiation and consideration on storage size," in *IEEE Trans. Sustainable Energy*, vol. 5, no. 1, 2014, pp. 171–181.

[65] R. S. Weissbach and J. R. King, "Estimating energy costs using a markov model for a midwest off-grid residence," in *in Proc. IEEE GTC*, 2013, pp. 430–434.

[66] D. Binkley and R. F. Fisher, "Ecology and management of forest soils." John Wiley & Sons, 2019.

[67] J. P. Walker, G. R. Willgoose, and J. D. Kalma, "In situ measurement of soil moisture: a comparison of techniques," in *Journal of Hydrology*, vol. 293, no. 1-4, 2004, pp. 85–99.

[68] O. Merlin, J. Walker, R. Panciera, R. Young, J. Kalma, and E. Kim, "Soil moisture measurement in heterogeneous terrain," in *Proc. Int. Congr. MODSIM*, 2007.

[69] W. Belisle, A. Sharma, and T. Coleman, "An optical reflectance technique for soil moisture measurement. i. theory, description, and application," in *IGARSS'96. 1996 International Geoscience and Remote Sensing Symposium*, vol. 2, 1996, pp. 1315–1319.

[70] V. S. Palaparthy, S. S. Lekshmi, J. John, S. Sarik, M. S. Bhagini, and D. N. Singh, "Soil moisture measurement system for DPHP sensor and in situ applications," in *2013 International Symposium on Electronic System Design*, 2013, pp. 11–15.

[71] O. Calla, D. Bohra, R. Vyas, B. S. Purohit, R. Prasher, A. Loomba, and N. Kumar, "Measurement of soil moisture using microwave radiometer," in *2008 International Conference on Recent Advances in Microwave Theory and Applications*. IEEE, 2008, pp. 621–624.

[72] C. K. Sahu and P. Behera, "A low cost smart irrigation control system," in *2015 2nd International conference on electronics and communication systems*. IEEE, 2015, pp. 1146–1152.

[73] G. J. Gaskin and J. D. Miller, "Measurement of soil water content using a simplified impedance measuring technique," in *Journal of Agricultural Engineering Research*, vol. 63, no. 2. Elsevier, 1996, pp. 153–159.

[74] A. Fares, H. Hamdhani, and D. Jenkins, "Temperature-dependent scaled frequency: Improved accuracy of multisensor capacitance probes," in *Soil Science Society of America Journal*, vol. 71, no. 3. Wiley Online Library, 2007, pp. 894–900.

[75] E. Veldkamp and J. J. O'Brien, "Calibration of a frequency domain reflectometry sensor for humid tropical soils of volcanic origin," in *Soil Science Society of America Journal*, vol. 64, no. 5. Wiley Online Library, 2000, pp. 1549–1553.

[76] W. Kunzler, S. G. Calvert, and M. Laylor, "Measuring humidity and moisture with fiber optic sensors," in *Sixth Pacific Northwest Fiber Optic Sensor Workshop*, vol. 5278. International Society for Optics and Photonics, 2003, pp. 86–93.

[77] S. K. Khijwania, K. L. Srinivasan, and J. P. Singh, "An evanescent-wave optical fiber relative humidity sensor with enhanced sensitivity," in *Sensors and Actuators B: Chemical*, vol. 104, no. 2. Elsevier, 2005, pp. 217–222.

[78] S. Muto, A. Fukasawa, T. Ogawa, M. Morisawa, and H. Ito, "Optical detection of moisture in air and in soil using dye-doped plastic fibers," in *Japanese journal of applied physics*, vol. 29, no. 6A. IOP Publishing, 1990.

[79] T. Seiyama, N. Yamazoe, and H. Arai, "Ceramic humidity sensors," in *Sensors and Actuators*, vol. 4. Elsevier, 1983, pp. 85–96.

[80] I. Long and B. French, "Measurement of soil moisture in the field by neutron moderation," in *Journal of Soil Science*, vol. 18, no. 1. Wiley Online Library, 1967, pp. 149–166.

[81] A. Samouëlian, I. Cousin, A. Tabbagh, A. Bruand, and G. Richard, "Electrical resistivity survey in soil science: a review," in *Soil and Tillage Research*, vol. 83, no. 2, 2005, pp. 173–193.

[82] D. Robinson, C. Campbell, J. Hopmans, B. K. Hornbuckle, S. B. Jones, R. Knight, F. Ogden, J. Selker, and O. Wendroth, "Soil moisture measurement for ecological and hydrological watershed-scale observatories: A review," in *Vadose Zone Journal*, vol. 7, no. 1, 2008, pp. 358–389.

[83] W. W. Verstraeten, F. Veroustraete, C. J. van der Sande, I. Grootaers, and J. Feyen, "Soil moisture retrieval using thermal inertia, determined with visible and thermal spaceborne data, validated for european forests," in *Remote Sensing of Environment*, vol. 101, no. 3, 2006, pp. 299–314.

[84] R. Sugiura, N. Noguchi, and K. Ishii, "Correction of low-altitude thermal images applied to estimating soil water status," in *Biosystems Engineering*, vol. 96, no. 3, 2007, pp. 301–313.

[85] S. Urban, M. Ludersdorfer, and P. Van Der Smagt, "Sensor calibration and hysteresis compensation with heteroscedastic gaussian processes," in *IEEE Sensors Journal*, vol. 15, no. 11. IEEE, 2015, pp. 6498–6506.

[86] L. O. Wijeratne, D. R. Kiv, A. R. Aker, S. Talebi, and D. J. Lary, "Using machine learning for the calibration of airborne particulate sensors," in *Sensors*, vol. 20, no. 1. Multidisciplinary Digital Publishing Institute, 2020, p. 99.

[87] Pedregosa and et al., "Scikit-learn: Machine learning in python," in *JMLR 12, pp. 2825-2830*, 2011.

[88] P. et al., "The pandas development team," in *pandas-dev/pandas: Pandas. Zenodo. doi:10.5281/zenodo.3509134*, 2020.

[89] W. McKinney and et al., "Data structures for statistical computing in python," in *Proceedings of the 9th Python in Science Conference*, vol. 445. Austin, TX, 2010, pp. 51–56.

[90] F. R. Hampel, "The influence curve and its role in robust estimation," in *Journal of the american statistical association*, vol. 69, no. 346. Taylor & Francis, 1974, pp. 383–393.

[91] M. K. Simon and M.-S. Alouini, "Digital communication over fading channels," vol. 95. John Wiley & Sons, 2005.

[92] A. Papoulis and S. U. Pillai, "Probability, random variables, and stochastic processes." 4th ed. McGraw-Hill.

[93] A. Muller, "Simulation of multipath fading channels using the monte-carlo method," in *Proceedings of ICC/SUPERCOMM'94 - 1994 International Conference on Communications*, vol. 3, 1994, pp. 1536–1540.

[94] G. Auer and et. al., "Cellular energy efficiency evaluation framework„" in *Proc. IEEE VTC (Spring)*, 2011.

[95] H. Mutlu and et. al., "Spot pricing of secondary spectrum usage in wireless cellular networks," in *Proc. IEEE INFO COM*, 2008.

[96] D. Melo and et. al., "Surprising patterns for the call duration distribution of mobile phone users," in *Machine learning and knowledge discovery in databases, Springer*, pp. 354–369.

[97] D. Willkomm and et. al., "Primary users in cellular networks: A large-scale measurement study," in *Proc. IEEE DySPAN*, 2008.

[98] in *https://sam. nrel. gov /, Last accessed: 2022.*

[99] in *http://www.nrel.gov/rredc/pvwatts/changing-param eters. htmldc2ac, Last accessed: 2022.*

[100] A. Maafi and A. Adane, "Analysis of the performances of the first-order two-state markov model using solar radiation properties," in *Renewable Energy*, vol. 13, no. 2, 1998, pp. 175–193.

[101] D. M. Pozar, "Microwave engineering," no. 2. 4th ed. Hoboken, NJ: John Wiley, 2012.

[102] T. Instruments, "Cc-antenna-dk2 quick start guide. [on- line] texas instruments," 2016.

APPENDIX A

ANTENNA PERFORMANCE MEASUREMENTS

The antenna selection and antenna tests are the important part of designing low cost and reliable wireless soil moisture sensor network systems. Performance of any wireless link can be measured by looking at packet loss over various distances. This is vital in determining the maximum potential sensor node spacing, which is a function of the range. Antenna choice makes a notable difference in range. High gain more expensive antenna provides longer range and fewer sensors required to cover a specific area with higher node cost, while lower cost antenna with lower gain increases the number of sensors required while lowering the cost per node. The trade-off between antenna gain, node cost, and number of sensors can be explored for each different scenario to find an optimum antenna choice for that particular channel model. Let us assume N represents the number of sensor nodes required in a network to cover a particular area of size $A \times A(m^2)$. With an antenna gain of G and range of $R(G)$, N can be written as

$$N = \left[\frac{A}{R(G)}\right]^2 \tag{A.1}$$

Assuming that node cost will also go up with gain, G, we define the node cost as $C(G)$ and total cost as

$$C_{total} = NC(G) = \left[\frac{A}{R(G)}\right]^2 C(G) \tag{A.2}$$

The performance of any wireless link can be measured by looking at packet loss over various distances. This is vital in determining the maximum potential sensor node resolution, which is function of the range. Two sensor nodes were used in this experimental test. First node was connected to a laptop acting as base station receiving data from the other node which is acting as sensor. RSSI and packet loss was measured at different distances as shown in figure A.1. The sensor node was configured to send 100 packets of random characters

at the desired center frequencies of 915 MHz. Once the transmission was complete, the second board was moved back to another distance (10, 50, 100, 150, 200, 250, and 300 ft) and transmission was repeated. These tests where also coupled with a review of the manufactures test data, with particular interest given to the directivity of the antenna, as well as the efficiency [101].

Antenna 1 as shown in figure A.2, was a CR2032 PCB Antenna [102], with an overall poor performance. It was the only antenna that the 300 ft tests results were not displayed, as there was such a significant gap in the test data due to poor transmission, that it was irrelevant to include in this report. Review of the manufacturer data showed a directivity of 4.25dBi, with an efficiency of 51.69% [102].

Antenna 2 in figure A.3, a chip antenna from Fractus Antennas™[102], preformed adequately. The manufacturer data was reviewed, and showed a directivity of 3.92dBi with an efficiency of 46.61% [102].

Antenna 3 as shown in figure A.4, a Compact PCB Helical Antenna [102], was the best preforming, showing the best potential to extend beyond the 300 ft range. Further review of the manufacturer data showed a directivity of 4.13 dBi, with an efficiency of 63.05% [102]. The first antenna tested, results shown above, was the antenna already included on the TI launchpad. Review of the manufacturer data showed a directivity of 4.61dBi, and an efficiency of 43.27%

Antenna 4 in figure A.5, was an array of two helical antennas placed orthogonal to each other for antenna diversity. It preformed similarly to antenna 3, and also provided a possibility for an extension in range. The manufacturer's test data showed a directivity of 4.39dBi, with an efficiency of 31.33% [102].

Antenna 5 was a PCB helical antenna which is shown in figure A.6. The worst performing, not quite reaching a 100 feet before falling below a level that was barely readable. Review of the manufacturer data gave a directivity of 4.16dBi, with an efficiency of 46.83%.

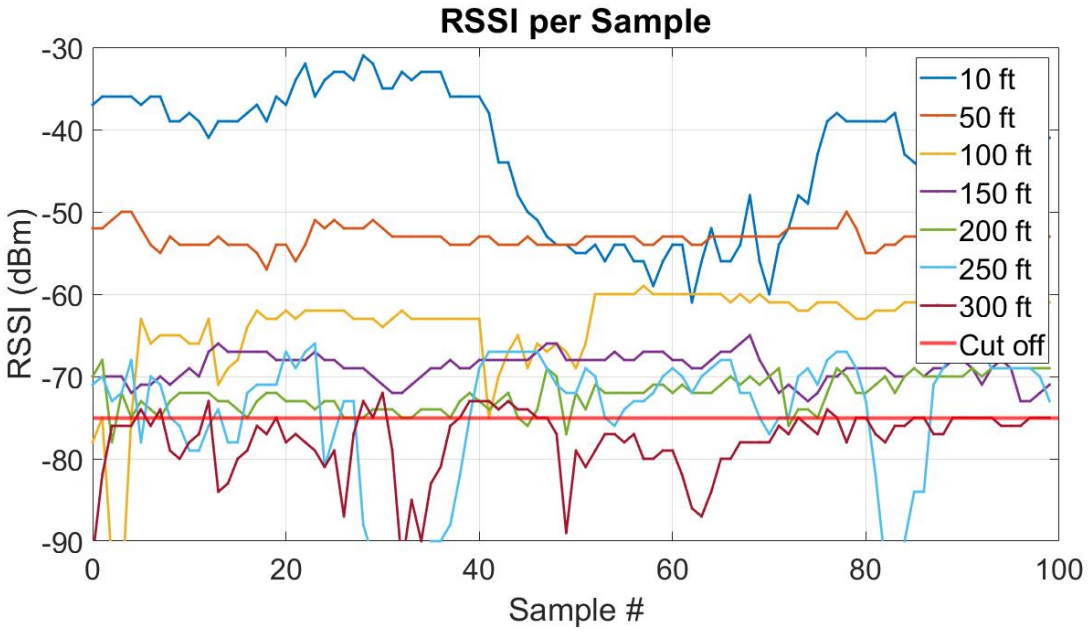

Figure A.1. RSSI at different distances with board antenna.

The best preforming antennas where antenna 3 and 4, with the built in board antenna coming along closely behind. Using a RSSI cut off value of -75dBm, the built in antenna achieved a working distance of 250 ft, and for now, we will use the 250 ft. result to design our network grid. However, the compact PCB helical demonstrated in antenna 3 will be implement to increase the 250 ft. range. The overall footprint of antenna 3 was smaller also compared to the built-in antenna, allowing for a more compact device in the future. Additionally, there is 19.78% in efficiency between the built-in antenna and antenna 3. Since the largest consumption of power in this device is from the transmissions, any improvements in this area would provide substantial impact to the length of operation and range of the device.

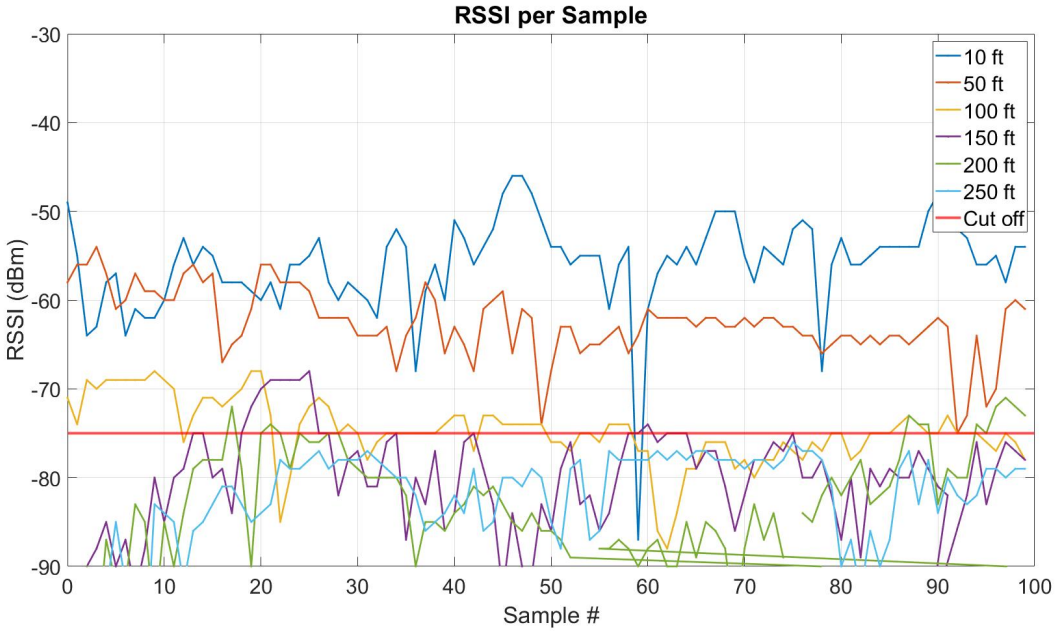

Figure A.2. RSSI at different distances with antenna 1

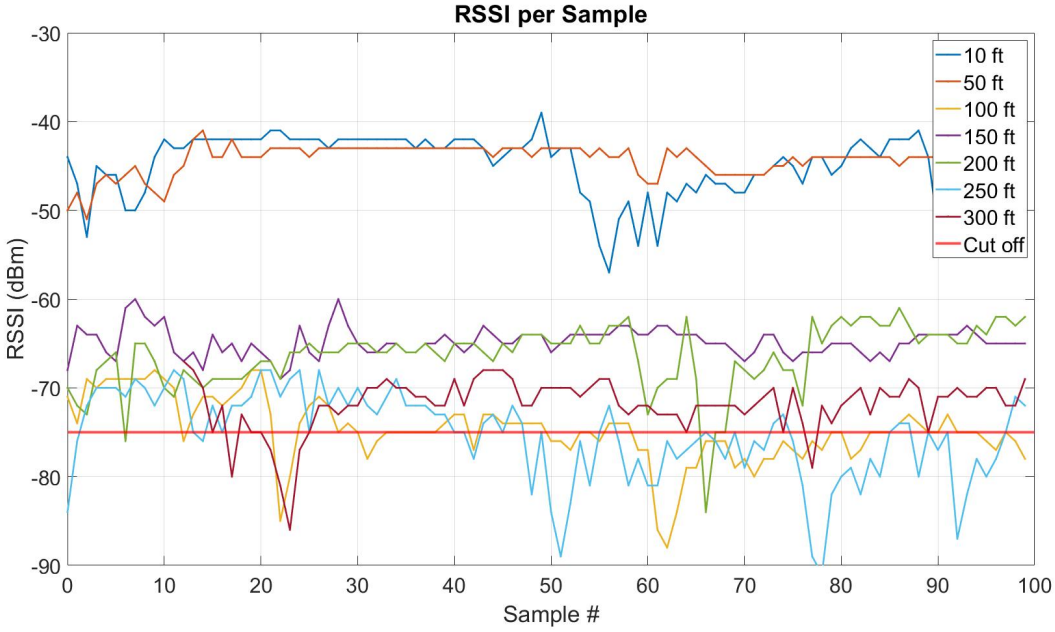

Figure A.3. RSSI at different distances with antenna 2

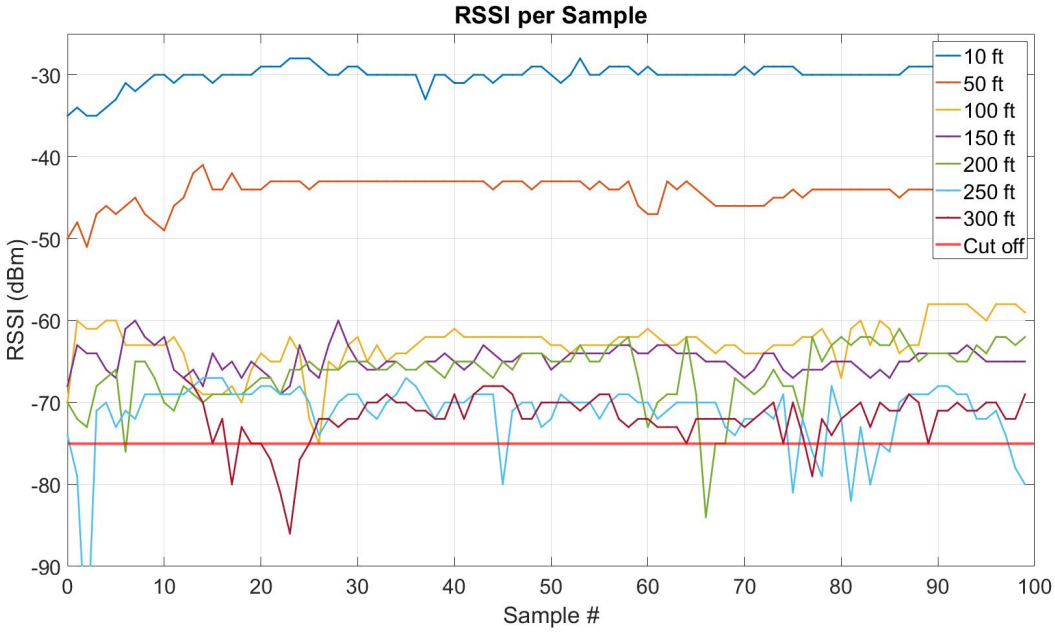

Figure A.4. RSSI at different distances with antenna 3

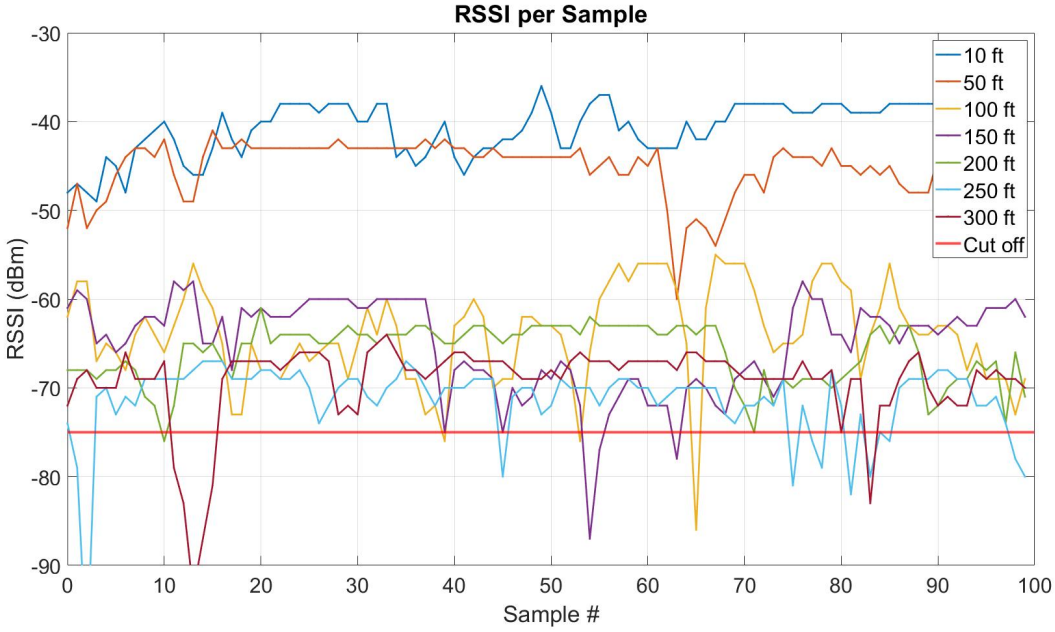

Figure A.5. RSSI at different distances with antenna 4

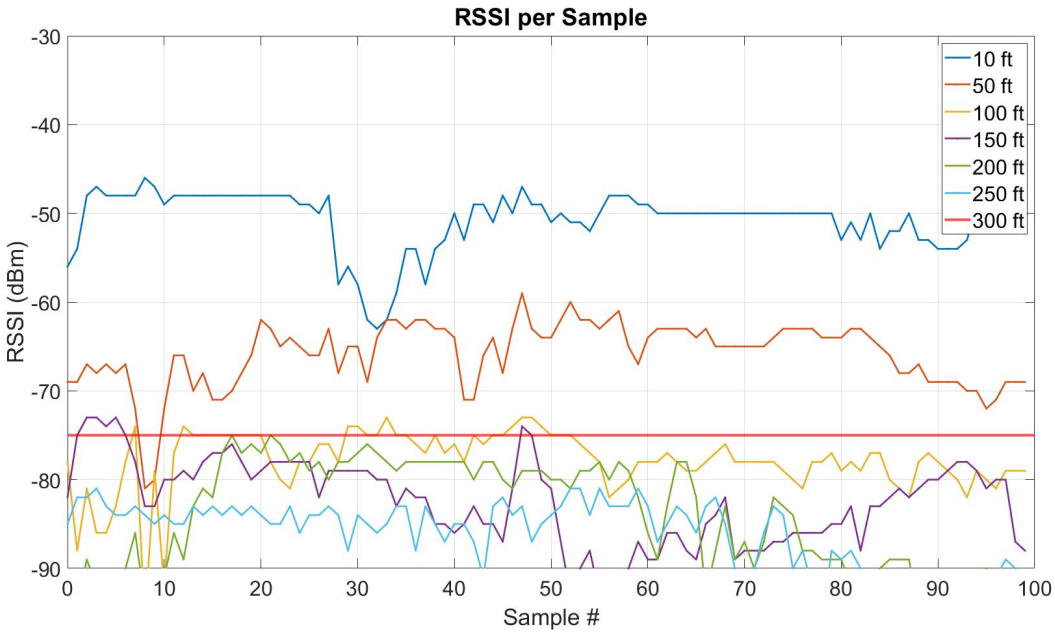

Figure A.6. RSSI at different distances with antenna 5

APPENDIX B

BATTERY LEVEL CALCULATION ALGORITHM

function $F(i)$
  if $1 \leq i \leq 2N$ **then**
    $S = S1$;
    $k = \lceil i/2 \rceil$;
  else if $2N + 1 \leq i \leq 4N$ **then**
    $S = S2$;
    $k = \lceil (i - 2N)/2 \rceil$;
  else
    $S = S3$;
    $k = \lceil (i - 4N)/2 \rceil$;
  end if
  if $i\%2 == 1$ **then**
    $L = L1$;
  else
    $L = L2$;
  end if
  initialize: $k' = k$, $O(i) = 0$
  for $t = 1 : 24$ **do**
    $k' = k' + E(t) - L(t)$;
    if $k' > K_{cap}$ **then**
      $k' = K_{cap}$;
    else if $k' < \nu K_{cap}$ **then**
      $k' = \nu K_{cap}$;
      $O(i) = 1$;
    end if
  end for
  return: $round(k')$
end function

Figure B.1. Algorithm 1: Battery level calculations

BIOGRAPHY OF THE AUTHOR

Sonia Naderi obtained her B.Sc and M.Sc degrees in Electrical Engineering from Shahrood University of Technology, Iran in 2008 and 2015, respectively. Since September 2018, she has been a PhD student in the Department of Electrical and Computer Engineering, University of Maine, Orono, USA. She was a research assistant at Wireless Sensor Networks (WiSe-Net) laboratory working under supervision of Dr. Ali Abedi (Aug2018-Aug2022). She passed her PhD candidacy exam successfully in September 2019.

She served as a treasure and chair of IEEE Women in Engineering Maine Section from 2019-2022. She was a Member of IEEE Maine section (2010-11). She has been awarded several IEEE conference travel grants from NASA and NSF during her PhD.

She joined Samsung Electronics America as a Wireless System Structure Design intern in the last summer of her PhD (Jun22-Aug22).

Her research focuses on wireless communication systems, wireless sensor networks, cooperative communication networks, information theory and channel coding and artificial intelligence.

Sonia Naderi is a candidate for the Doctor of Philosophy degree in Electrical Engineering from the University of Maine in August 2022.